

ISTANBUL TECHNICAL UNIVERSITY ★ GRADUATE SCHOOL OF
SCIENCE ENGINEERING AND TECHNOLOGY

DETACHMENT OF NANOPOROUS ANODIC ALUMINA MEMBRANES
FROM ALUMINIUM SURFACE

M.Sc. THESIS

Emek Göksu DURMUŞOĞLU

513101005

Department of Nanoscience and Nanoengineering

Nanoscience and Nanoengineering Programme

Thesis Advisor: Prof. Dr. Mustafa ÜRGEN

AUGUST 2012

İSTANBUL TEKNİK ÜNİVERSİTESİ ★ FEN BİLİMLERİ ENSTİTÜSÜ

**NANOPORUZ ANODİK ALÜMİNA MEMBRANLARIN ALÜMİNYUM
YÜZEYİNDEN AYIRILMASI**

YÜKSEK LİSANS TEZİ

Emek Göksu DURMUŞOĞLU

513101005

Nanobilim ve Nanomühendislik Anabilim Dalı

Nanobilim ve Nanomühendislik Programı

Tez Danışmanı: Prof. Dr. Mustafa ÜRGEN

AĞUSTOS 2012

Emek Göksu DURMUŞOĞLU, a **M.Sc.** student of ITU **GRADUATE SCHOOL OF SCIENCE ENGINEERING AND TECHNOLOGY** student ID 513101005, successfully defended the **thesis** entitled “**Detachment of Nanoporous Anodic Alumina Membranes from Aluminium Surface**”, which he prepared after fulfilling the requirements specified in the associated legislations, before the jury whose signatures are below.

Thesis Advisor : **Prof. Dr. Mustafa ÜRGEN**

Istanbul Technical University

Jury Members : **Doç. Dr. Kürşat KAZMANLI**

Istanbul Technical University

Doç. Dr. Nuri SOLAK

Istanbul Technical University

Date of Submission : 20 July 2012

Date of Defense : 14 August 2012

FOREWORD

I would like to thank to my supervisor Prof. Dr. Mustafa ÜRGEN for his guidance throughout the period of my thesis studies. I am very much thankful to Res. Assist. Beril AKINCI, Seyhan ATİK, Fatma BAYATA, Sinem ERASLAN, Talat ALPAK for their tremendous support and guidance.

My special thanks goes to my mother Müzeyyen DURMUŞOĞLU, my father Haluk DURMUŞOĞLU, Gökay DURMUŞOĞLU and Esra NESİPOĞULLARI who have never lost their belief in me and to my friends for keeping me motivated at all times.

August 2012

Emek Göksu DURMUŞOĞLU
(Metalurgy and Material Engineer)

TABLE OF CONTENTS

	<u>Page</u>
.....	v
FOREWORD	vii
TABLE OF CONTENTS	ix
ABBREVIATIONS	xi
LIST OF TABLES	xiii
LIST OF FIGURES	xv
SUMMARY	xix
ÖZET	xxi
1. INTRODUCTION	1
2. NANOPOROUS ANODIC ALUMINA	5
2.1 Definition	5
2.2 Two-Step Anodization	9
2.2.1 Pore diameter	13
2.2.2 Interpore distance	18
2.2.3 Wall thickness	19
2.2.4 Barrier layer thickness	19
2.2.5 Oxide removal	22
2.3 Detachment of NPAA from Aluminium Surface	23
3. EXPERIMENTAL STUDIES	29
3.1 Experimental Method	29
3.2 Electropolishing	30
3.3 Two-Step Anodization	30
3.4 Detachment of NPAA Membrane	30
4. RESULT AND DISCUSSION	33
5. CONCLUSION	47
REFERENCES	49

ABBREVIATIONS

NPAA	: Nano Porous Anodic Alumina
AAO	: Anodized Aluminum Oxide
TEM	: Transmission Electron Microscope
SEM	: Scanning Electron Microscope
MBE	: Molecular Beam Epitaxy
MEMS	: Micro Electromechanical Systems
FEG-SEM	: Field Emission Gun Scanning Electron Microscope
STEM	: Scanning Transmission Electron Microscope

LIST OF TABLES

	<u>Page</u>
Table 1.1: Properties of Anopore Membranes by their types (Url-2).....	3
Table 2.1: Major acid components of typical electrolyte types used to produce porous oxide layer on an aluminum substrate (Poinern, 2011).....	13
Table 2.2: Geometric parameters of the hexagonal pore array (Sui, 2001)	18
Table 2.3: Anodizing ratio (B_U) for various anodizing electrolytes (Sulka, 2008).	21
Table 2.4: Detaching results and the corresponding parameters of some electrolytes (Yuan, 2006).	27
Table 3.1: Anodization Parameters.	31
Table 4.1: Comparison of empirical and therotical datas of pore diameter (nm).	35
Table 4.2: Comparison of empirical and therotical datas of interpore dinstance (nm).	36
Table 4.3: Comparison of empirical and therotical datas of wall thickness(nm).	37

LIST OF FIGURES

	<u>Page</u>
Figure 1.1 : The structure and the pore shape of Anopore membrane	2
Figure 2.1 : TEM picture of anodic alumina	5
Figure 2.2 : (a) Idealized structure of anodic porous alumina and (b) a cross-sectional view of the anodized layer	6
Figure 2.3 : Schematic representation of the experimental setup.....	8
Figure 2.4 : Two step anodization steps a) Electropolished surface, b) First anodization, c) Oxide removal, d) Second anodization	10
Figure 2.5 : FEG-SEM image of two-step anodized AAO structure with 30 nm pore diameter obtained in 0.3 M oxalic acid solution with 15 °C and 40 V: (a) side and top view, (b) macroscopic distribution of pores in a random fashion.....	11
Figure 2.6 : STEM image of AAO structure: (a) AAO structure after the second anodization step (no widening; diameter: about 30 nm); (b) an enlarged image of (a);	12
Figure 2.7 : Influence of voltage upon AAO layer thickness	12
Figure 2.8 : Parameters these have influence on pore diameter	14
Figure 2.9 : Effect of electrolyte temperature on anodization	16
Figure 2.10 : Effect of stirring on the pore diameter of nanostructures obtained by anodization of aluminum (Sulka, 2008)	17
Figure 2.11 : Anodizing potential influence on the barrier layer thickness for anodic porous alumina formed in sulfuric, oxalic, glycolic, phosphoric, tartaric, malic, and citric acid solutions (Chu, 2006).....	22
Figure 2.12 : Top view FESEM images of AAO templates prepared by using different etching times (a) 5 min (b) 15 min (c) 30 min (d) 60 min (Erdogan, 2012)...	23
Figure 2.13 : Schematic representation of the fabrication procedure for the formation of ordered and through-hole porous alumina membrane. (A) Formation of the porous alumina layer after the first anodic oxidation process; (B) removal of the porous alumina layer; (C) formation of the ordered porous alumina layer after the second anodic oxidation process; (D) free-standing PAA; and (E) the barrier layer structure on aluminum base after electrical detachment of the PAA (Yuan, 2004).	25

Figure 2.14: Effect of different detaching voltage (*) 5+40V; (□) 5+30V; (●) 10+40V; (×) 0 + 40V on the current density in a solution of 70% HClO ₄ + 98% CH ₃ COCOCH ₃ (v/v = 1:1) at 25 °C for 3 seconds. The PAA film–Al hybrids were formed at different anodic oxidation voltage (40 or 30 V) in a 0.3M H ₂ C ₂ O ₄ solution at 25 °C for 4 hours (Yuan, 2006).	26
Figure 2.15: SEM images of (a) the surface and (b) the bottom view of the through-hole PAA membrane detached at 70 V for 3 s in 1:1 HClO ₄ + ethanol mixture. Bottom images of the PAA membranes detached at (c) 65 V, (d) 62 V, (e) 60 V, (f) 59 V. The PAA was formed at 60 V in a 0.3M oxalic acid and the thickness was 70 μm (Chen, 2006).	28
Figure 2.16: Dependence of the open pores diameter on the detaching voltage (Chen, 2006).	28
Figure 3.1: Experiment Scheme	29
Figure 4.1: (a) FEG-SEM image of NPAA produced with one-step anodization in 0.3 M C ₂ H ₂ O ₄ for 1 hour at 40 V, (b) FEG-SEM image of NPAA after two-step anodization using the same anodization parameters.	34
Figure 4.2: FEG-SEM images of NPAA membranes produced by two-step anodization in 0.3 M C ₂ H ₂ O ₄ for 5 min. at (a) 40 V, (b) 50 V, (c) 60 V.	34
Figure 4.3: Influence of Voltage to Morphology	35
Figure 4.4: Influence of Voltage to Interpore Dinstance	36
Figure 4.5: Influence of Voltage to Wall Thickness	37
Figure 4.6: FEG-SEM cross-section image of NPAA membrane under the second anodization 0.3 M C ₂ H ₂ O ₄ at 40 V for (a) 1 hour, (b) 2 hours, (c) 3 hours	38
Figure 4.7: FEG-SEM cross-section image of NPAA membrane under the second anodization in 0.3 M C ₂ H ₂ O ₄ at 60 V for (a) 1 hour, (b) 2 hours, (c) 3 hours	39
Figure 4.8: Influence of Anodization Time to Membrane Thickness	39
Figure 4.9: FEG-SEM image of NPAA membrane under the second anodization in 0.3 M C ₂ H ₂ O ₄ for 5 min. at (a) 100 rpm, (b) 500 rpm, (c) 900 rpm	40
Figure 4.10: Influence of Stirring Speed to Pore Radius.....	41
Figure 4.11: Influence of Stirring Speed to Wall Thickness	41
Figure 4.12: Influence of Stirring Speed to Interpore Distance	42
Figure 4.13: FEG-SEM cross-section image of NPAA membrane under the second anodization 0.3 M C ₂ H ₂ O ₄ at 40 V for 5 minutes at (a) 100 rpm, (b) 500 rpm, (c) 900 rpm.....	43
Figure 4.14: Influence of stirring Speed to Membrane Thickness.....	42

Figure 4.15: FEG-SEM image of etched AAO surface in chromic-phosphoric acid mixture for 1 hour at 60 0C at (a) 40 V, (b) 60 V.....	44
Figure 4.16: Detachment surfaces of different NPAA, these obtained at different voltages; (a) 40 V, (b) 60 V, (c) 70 V	45
Figure 4.17: Two-step anodized samples at 60 V for one hour and detached at 70 V. (a) top surface, (b) detachment surface before etching; (c) detachment surface after etching with 0.1 M mixture of 1.8% CrO ₃ and 7.1% H ₃ PO ₄ acid for 5 minutes	46

DETACHMENT OF NANOPOROUS ANODIC ALUMINA MEMBRANES FROM ALUMINIUM SURFACE

SUMMARY

In nanoscale size, many materials start to behave in different ways. They can become much stronger, or conduct more electricity; opaque substances can become transparent, solids become liquids at room temperature or insulators become conductors. This often occurs because of their increasing surface to volume ratio because of their decreasing size.

Recent progresses on nanomaterials have made porous nanostructures a particularly interesting class of materials for both scientific and technological explorations. Because of their intricate nanostructures, extremely big surface-volume ratio, low dimensionality and interplay among constituents, they often exhibit new and enhanced properties than bulk materials. There are commercially available processes and materials available in the market both for producing and marketing nanoporous structures. Anodic oxidation (anodization) of aluminium in nanoporous form is one the most widely used process for producing nano sized templates.

Anodization is an electrochemical process using for growing an oxide layer on certain metals – aluminium, niobium, tantalum, titanium, tungsten, and zirconium. At certain conditions of anodization process –generally in acidic solutions-, it is possible to fabricate this oxide layer as a self-ordering porous structure.

Due to their low-cost and easy fabrication, nanoporous membranes like nanoporous anodic alumina are commonly using for the fabrication of very high aspect ratio structures. The ratio of the thickness of membrane and diameter of the pores can be very large in NPAA. This property makes NPAA very suitable for fabrication of nanostructures such as nanowires and nanorods. Nowadays, although several companies commercially produce NPAA membranes for research and industrial applications, researchers prefer to produce their AAO membranes themselves thus there is a continuing effort in developing the methodology of AAO membrane production. There are basically two routes for the production of free standing AAO membranes:

1. Chemical processes based on selective dissolution of left behind metallic aluminum after the anodization process
2. Electrochemical detachment process which relies on local rapid dissolution of barrier layer and metallic aluminum below.

Although the chemical processes based on selective dissolution is very well known the requirement of highly toxic chemicals makes it a difficult process for applications. Electrochemical detachment method is a more environmentally friendly alternative to chemical dissolution process in which dissolution of the remnant aluminum is not required.

However the role of anodic oxidation parameters on the character of the detached film has not been systematically investigated

The aim of this study to investigate the parametric relations in the electrochemical detachment process. The method used, is based on two-step anodization for obtaining self-ordered nanoporous aluminium oxide membranes and then detaching the membrane by using of perchloric-ethanol mixture from the aluminium surface. The role of anodic oxide structure obtained by the application of different anodization voltages, stirring speed and time on the detached film character.

The results of the study demonstrated that the anodic oxide character affected the barrier layer perforation morphologies, which eventually leads to the detachment of the film.

NANOPOROZ ANODİK ALÜMİNA MEMBRANLARIN ALÜMİNYUM YÜZEYİNDEN AYIRILMASI

ÖZET

Nanoteknoloji geçtiğimiz yüzyılın en önemli gelişmelerinden biri kabul edilmektedir. Nanoteknoloji sayesinde insanoğlu yeni mühendislik uygulamaları için çok önemli bir alanı control edebilir hale gelmiştir. Nano kelimesi köken olarak Latince'den gelir ve 'cüce' anlamına gelir. Kelimenin tanımından da anlayabileceğimiz üzerine nano teknolojinin alanına maddenin küçük boyutluları girer. Yani nanometre bir ölçü birimidir ve metrenin milyarda biridir. Bir metreyi aklımızda canlandırmak pek sorun olmayacaktır çünkü günlük yaşantımızda uzunluğu genelde metre üzerinden hesaplarız. Ama bir kilometre veya bir milimetre biraz daha zor olacaktır ve metrenin milyarda biri kolay kolay aklımızda canlandırabileceğimiz bir şey olmayacaktır. Bu nedenle bu noktada bilimsel bir yöntem olarak karşılaştırma daha uygun olacaktır. Bir nanometre (nm) genelde yaklaşık 10 atomun uzunluğudur (1 atom 1-4 angstrom çapındadır), DNA 2 nm, virüsler 100 nm, bakteriler 1000nm (1 mikrometre), kan hücreleri 2-5 mikrometre, saç telinin çapı 100 mikrometre, iğnenin başı ise 1 mm'dir.

Nanoteknolojinin özel olmasının yani 1-100 nm arasındaki boyutun özel bir anlam içermesinin sebebi malzemelerin bu boyut arasında olağandışı özelliklerinin vuku bulmasıdır. Nano boyutta birçok malzeme normalden farklı davranışlar gösteriyor. Daha sağlam olabiliyorlar veya daha fazla iletken olabiliyorlar; opak maddeler transparan, katılar oda sıcaklığında sıvı olabiliyor veya yalıtkanlar iletken hale gelebiliyorlar. Bu genellikle maddenin küçülen boyutuyla birlikte büyüyen yüzey-hacim oranından kaynaklanıyor. Nano boyutta malzemelerin niteliksel olarak gösterdikleri farklılıklar için altın önemli bir örnektir. Altının bir külçe altınla, bir gram ve nokta kadar bir altın aynı kimyasal ve yaklaşık fiziksel özellikleri gösterir; yani parlak sarı renklidir, elektriği ve ısıyı iyi iletir vs. Ama altını daha küçültüp nanometre düzeyine getirdiğimizde olağanüstü bir durum ortaya çıkıyor ve altın mavi, pembe veya diğer renklerde olabiliyor ve bunula birlikte diğer tüm özellikleri de boyutuyla beraber değişmeye başlıyor.

Nanoteknoloji ilgi alanı olan maddenin yaklaşık 100 nm'den daha küçük boyutları genel olarak maddenin niteliğinin değişmeye başladığı boyut olarak kabul edilir ve biz bu alana (0.1-100 nm) maddenin kuantum özelliklerinin açığa çıktığı alan diyoruz. Nano teknolojinin uğraşlarından biri maddenin kuantum özelliklerinin ortaya çıktığı 1-100 nm aralığında araştırmalar yapmaktır. Tabii araştırmakla kalması hayatlarımızda pek bir şeyi değiştirmezdi, nano teknoloji bununla beraber bu boyutlardaki maddeyi kontrol ve manipüle edebilmemizi ve bu boyutlarda ortaya çıkan olağandışı özellikleri proseslere uygulayabilmemizi sağlar.

Atomsal düzeydeki malzemelerin amaca yönelik yapılandırılmalarında ve bu kadar küçük boyuttaki özel görüngülerden yararlanma birçok alanda yeni imkânların doğmasına yol açmıştır. Bu alanlardan bazıları şunlardır: Enerji, çevre tekniği, IT- Branşı, Tıp, Eczacılık vs. Atomsal düzeyde kimya, biyoloji ve fizik arasında sınır yoktur.

Nanobilim yeni malzemeler üretmenin yanında, yeni malzemeler üretebilmek için gerekli olan uygulamaları üretebilmemizi de sağlıyor. Nanomalzemeler konusunda elde edilen son gelişmelerle birlikte poroz nanoyapıları hem bilimsel hem teknolojik araştırmalar için ilginç bir malzeme sınıfı haline getirdi. Nanoporoz yapılar, girintili çıkıntılı yapıları, aşırı derece büyük yüzey-hacim oranları, küçük boyutları ve içeriklerin karşılıklı etkileşimi nedeniyle, çoğunlukla bulk yapılara göre yeni ve gelişkin özellikler gösterirler. Nanoyapılı malzemelerin hem üretimi hem de pazarlaması için prosesler ticari olarak bulunmaktadır. Alüminyumun nanoporoz formda anodik oksidasyonu (anodizasyon) nanoboyutlu kalıpların üretilmesinde en yaygın olarak kullanılan yöntemlerden biridir.

Anodizasyon, alüminyum, niyobyum, tantalyum, titanyum, tungsten, zirconyum gibi belli metallerin üzerinde oksit tabakası büyütmek amacıyla kullanılan elektro-kimyasal bir yöntemdir. Anodizasyon prosesinin belli koşullarında –genellikle asidik çözeltilerde-, bu oksit tabakasını kendiliğinden düzenlenen poroz yapı olarak elde etmek mümkündür. Bu tezde bu poroz yapının morfolojik özellikleri üzerinde çalışılmıştır.

Alüminyumun poroz anodize yapısı kendiliğinden düzenlenebilir altıgenler şeklinde dizilirler. İki adım anodizasyon işlemi ile elde edilen anodik alümina yapısal olarak çok düzgün bir dizilime sahiptir. Anodize yapılar por çapı, porlar arası mesafe, duvar kalınlığı ve membran kalınlığı gibi anodizasyon koşullarına ve birbirlerine göre değişen birçok yapısal özelliğe sahiptirler. Bu özelliklere etki eden parametreleri anodizasyon potansiyeli, süresi, sıcaklığı, karıştırma, kullanılan çözelti olarak sayabiliriz. Bu çalışmada bu parametrelerin morfolojik yapıya etkileri incelenmiştir.

Düşük maliyeti ve kolay üretimleri nedeniyle, nanoporoz anodik alümina gibi nanoporoz membranlar çok yüksek en-boy oranlı yapıların üretimi için yaygın olarak kullanılırlar. NPAA’larda pore çapı ile membranın kalınlığı arasındaki oran çok yüksek olabilir. Bu özellik nedeniyle NPAA, nanoteller ve nanoçubuklar gibi yapıların üretimi için çok uygundur. Bugünlerde, NPAA membranlar birkaç şirket tarafından araştırma ve endüstriyel uygulamalar için ticari olarak üretiliyorlar. Okside yapıyı alüminyum üzerinde büyütmek kolay bir yöntemken NPAA membranları alüminyum üzerinden ayırma işlemi bu konuda çalışma yapan bir çok bilim grubu uzun süreli olarak meşgul etmiş bir problemdir. Bugün, NPAA membranları ayırma işleminde kullanılan iki tane yöntem vardır;

1. Anodizasyon prosesi ardından kimyasal olarak selektif çözüme ile alüminyum metalini elde etme.
2. Bariyer tabakasını hızlıca çözerek geriye metalik alüminyumu bırakan elektrokimyasal ayırma prosesi.

Selektif çözüme dayanan kimyasal çok iyi bilinen bir yöntem olmasına rağmen proses için gerekli kimyasalların yüksek toksik olması prosesi uygulamam için zorlaştıran bir

etken. Elektrokimyasal ayırma yöntemi, kimyasal çözme prosesine göre daha çevre dostu bir alternatiftir ve ayrıca kimyasal çözmede olduğu gibi kalan alüminyumun çözülmesini gerektirmez. Bunun yanında elektrokimyasal ayırma yöntemi çok daha hızlı ve basit bir yöntemdir. Bu nedenle bu tezde elektrokimyasal ayırma yönteminin özellikleri incelenecektir. Biraz önce verilen avantajlara rağmen anodik oksidasyonun parametrelerinin ayrılan film üzerindeki etkisi sistematik olarak henüz incelenmemiştir.

Bu çalışmanın hedefi elektrokimyasal çözme işlemindeki parametrik ilişkilerin incelenmesidir. Bu çalışma kendiliğinden düzenlenen nanoporoz alüminyum oksit membranların elde edilmesi ve daha sonra membranın perklorik-ethanol karışımı kullanılarak alüminyum yüzeyinden ayrılmasına dayanıyor. Ayrılma filminin karakteri üzerindeki anodik oksit yapının rolü, değişik anodizasyon voltajı, karıştırma hızı ve zamanı kullanılarak ölçülmüştür.

Bu çalışmanın sonuçları anodik oksit yapının karakterinin bariyer katmanın morfolojisini etkilediğini ve bununda kaçınılmaz olarak ayrılan filmin yapısını değiştirdiğini göstermiştir.

1. INTRODUCTION

Nanotechnology is an advanced technology involving the fabrication and use of devices so small that the convenient unit of measurement is nanometers. This technology, which is being used since the ancient times, continues to surprise researchers nowadays with every single unveiled findings (Url-1).

The discovery of anodic oxidation began at the last century and firstly it used cosmetic purposes and anticorrosion applications as a protective surface. Anodic oxidation used for obtaining barrier layers in early products. Then hexagonal porous structure discovered in the early 80's. Although anodization once done on aluminium for surface protection, with the discovery of this self-ordered structure, scientists started to use this unique material for nanotechnological applications (Choi, 2004).

For anodization process scientist used many different anodization baths according to the needs. Anodization studies shows that anodization parameters and electrolyte are changing the morphology of the porous structure. Bengough and Stuart's patent in 1923 was a break-through in anodic oxidation field which provided a way to protect Al and its alloys against corrosion by anodizing in chromic acid bath (Choi, 2004; Huh, 2007).

Although there are many papers, research is still continuing to enhance and optimize the anodization process. Especially after the developments made in scanning electron microscopy, researches on these topics showed a great increase. O'Sullivan and Wood researches took great attention in this field, which was an important step for a better understanding of oxidation morphology and mechanism (O'Sullivan, 1970; Choi, 2004).

Another important discovery about anodization was Masuda and Fukuda's report about an ordered pore arrangement in an anodic aluminium oxide (AAO). AAO

template gains a wide use accept in nanotechnology area after their work. AAO template is an ideal mold because it possesses many desirable characteristics, including tunable pore dimensions, good mechanical property, and good thermal stability (Masuda, 1995).

Moreover, especially for metal nanowires, the nanoporous anodic alumina (NPAA) membrane is a cheap and high yield technique that allows producing large arrays of metals nanowires by the electrodeposition. NPAA has ordered hexagonal cells and every cell contains a cylindrical pore at its center. The pore diameter, cell size and barrier layer thickness can be controlled by anodizing voltage and the depth of pore by anodizing time (Hamrakulov et al., 2009).

After recent developments on well-ordered surface, state of the art NPAA with honeycomb architecture is mainly used as a template for the production of one-dimensional nanomaterials.

After obtaining stable NPAA membranes and optimizing the fabrication process, companies begin to offer NPAA products for the synthesis of nanostructures. Product of Whatman Company, Anopore membranes are one of the good examples of this. Figure 1.1 shows the structure and the pore shape of Anopore membrane and table 1.1 shows the properties of Anopore membrane by theirs types. According to Whatman company, these membranes can be used in filtration and degassing, ultra cleaning of solvents, gravimetric analysis, liposome extrusion, scanning electron microscopy studies, bacterial analysis by epifluorescence light microscopy, micrometer and nanometer filtration and metal nanorods formation applications (Url-2).

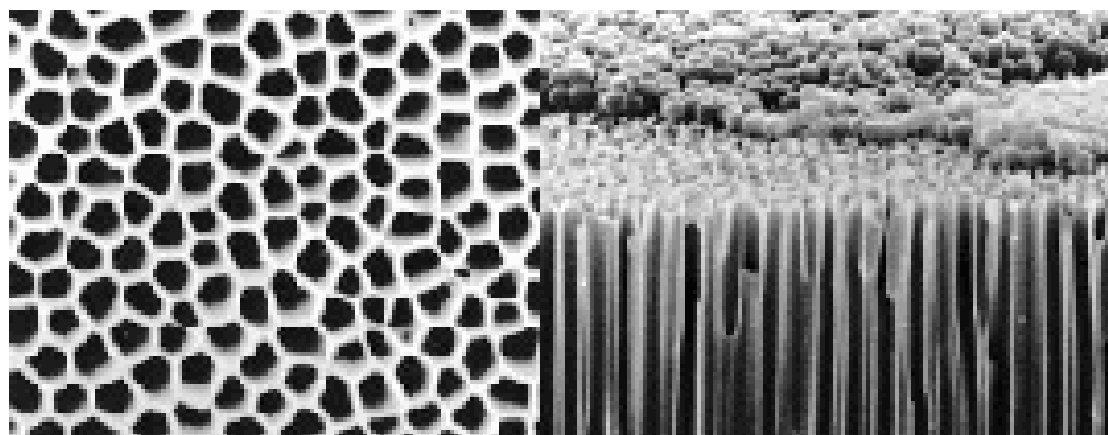


Figure 1.1: The structure and the pore shape of Anopore membrane (Url-2).

Table 1.1: Properties of Anopore Membranes by their types (Url-2).

Typical Data - Anopore Inorganic Membranes			
	Anodisc 13	Anodisc 25	Anodisc 47
Average membrane thickness	60 μm	60 μm	60 μm
Membrane diameter	13 mm	21 mm	43 mm
Membrane type	Anopore aluminum oxide	Anopore aluminum oxide	Anopore aluminum oxide
Support ring material	None	Polypropylene	Polypropylene
Construction process	None	Thermal weld	Thermal weld
Protein adsorption	Low	Low	Low
Burst strength	65 to 110 psi	65 to 110 psi	65 to 110 psi
Maximum service temperature	400°C	40°C	40°C
Porosity	25 to 50%	25 to 50%	25 to 50%
Autoclavable	Yes	No	No
Refractive index	1.6	1.6	1.6

While the number of membrane products is increasing and production process becomes regular, the number of research papers is increasing constantly. One of the main research areas is the use of these membranes as a template for controlled production of the nanostructures.

Improvements in the area of one-dimensional nanomaterials attracted very wide attention due to the unique properties and potential application in the ultrahigh-density magnetic memories, optoelectronic devices and micro sensors. A general approach of nano-fabrication that utilizes the self-organized, highly ordered NPAA membrane as template, combined with electrodeposition or sol-gel method, is employed to synthesize vastly different nanoarrays, such as metal, semiconductor and conducting polymer (Zhou et al., 2007).

2. NANOPOROUS ANODIC ALUMINA

2.1 Definition

Anodizing is an electrochemical process, which is performed to form a protective oxide layer on the surface of a metal. An oxide film can be grown on certain metals – aluminum, niobium, tantalum, titanium, tungsten, and zirconium. It is a method to grow a controlled oxide layer rather than a naturally formed metal oxide. The finish product of anodizing process is called anodic oxide (Fig. 2.1). This oxide layer can be used for enhancing corrosion resistance or wear resistance for increasing surface hardness or even obtaining a different appearance. Utilizing this process allows us to use a metal in applications for which it might not otherwise be suitable for the area of use. (Url-3; Choi, 2004)

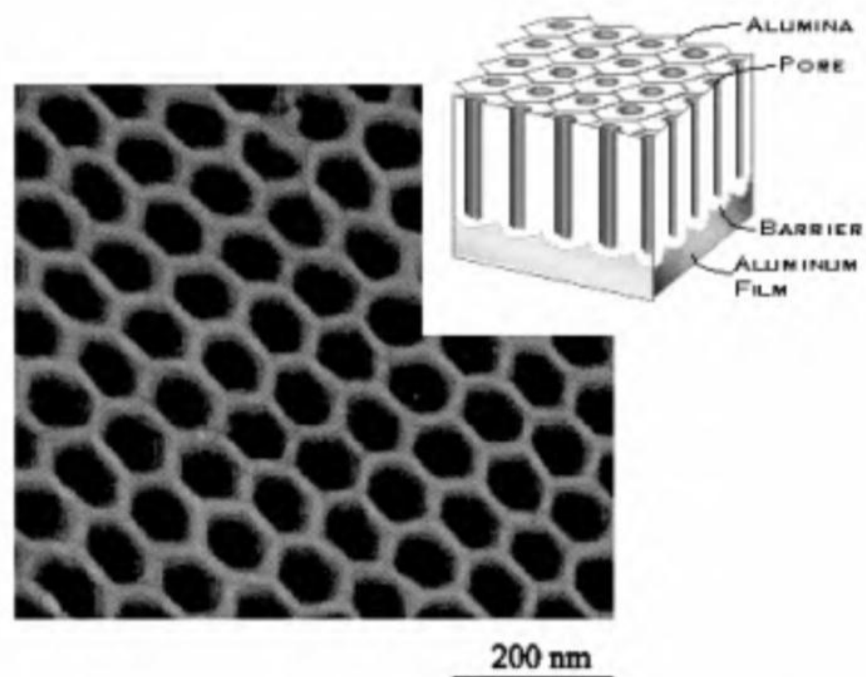


Figure 2.1: TEM picture of anodic alumina (Zheng et al., 2001).

Anodization of aluminium as a surface finish offers wide range of advantages such as increasing the durability, corrosion and wear resistance and decorative appeal. Moreover, low cost and ease of fabrication makes it a highly preferable material for these applications.

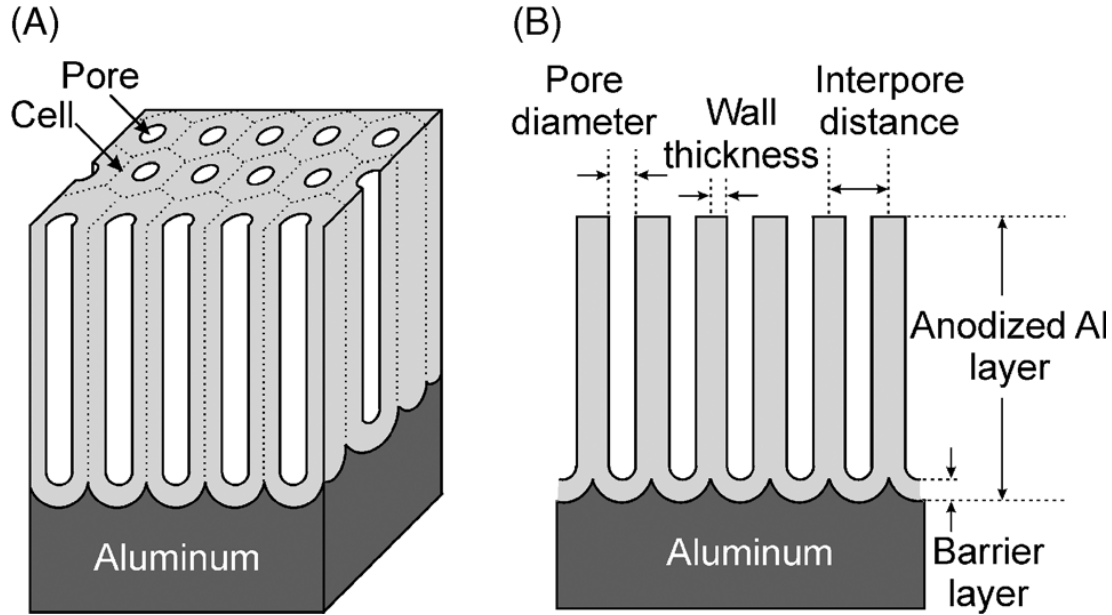


Figure 2.2: (a) Idealized structure of anodic porous alumina and (b) a cross-sectional view of the anodized layer (Sulka, 2006).

Because of the nature of aluminium metal, during anodization, porous anodic aluminium oxide (AAO) forms on it. While the anodized aluminum has been used as anticorrosion or decoration coating to improve the mechanical and corrosion properties of aluminium, the nanoporous anodic aluminium (NPAA) is now widely employed in nanoscience and nanotechnology as membrane for its self-ordered uniform cylindrical pore size and pore density (Han, 2011). NPAA has been extensively used as template, mask, or host materials to synthesize various nanostructures in the form of nanopores, nanowires, nanotubes, and nanodots, which are all functional materials for developing nanoscale devices. Fig. 2.2 shows idealized structure of AAO and a cross-sectional view of the anodized layer. At surface, there are hexagonal cells and cylindrical pores inside the cells. At cross-section, we can see tube-shape structure and barrier layer, pore diameter, wall thickness and interpore distance. This porous structure can be produced on a wide surface. Depending on the production method, it can be highly ordered.

Porous structure also creates a possibility to use AAO as templates for filling them with different materials such as Nickel, Silver, Gold etc. (Choi, 2004) utilizing different coating methods for filling the pores.

The two-step anodization process for obtaining self-ordered alumina nanostructures was mentioned for the first time in 1995. This improvement has led to an increase on the usage of these materials as membranes due to its easy and relatively low cost (Moldavan, 2011; Hagelsieb, 2007).

Anodization is a very simple oxidation process employed in a two-electrode electrochemical cell consisting of an anode (aluminium or aluminium alloy), a cathode (stainless steel or platinum), DC or AC power supply and an electrolyte. To obtain nanoporous membranes by anodization, the process was carried out on the experimental setup (Fig. 2.3), composed of electrical source (1), measurement devices (2), thermometer (3), reference electrode (4), Al substrate (5), thermo insulating outer vessel (6), Cu spiral (7), mechanical stirrer (8), anodizing tank (9), cathode (10). By applying direct current, a controlled growth of oxide layer on surface of the anode is achieved where the surface is in contact with the electrolyte. Anodic oxide structure is not applied onto the surface as a film. Unlike electroplating, it is a surface finish, which originates from the base metal itself by turning the metal into its oxide (e.g. Al to Al_2O_3). As in case of anodic aluminium oxide (AAO), the oxide layer is fully integrated with aluminium underneath, which prevents it from being peeled or chipped. (Hagelsieb, 2007; Choi, 2004; Pasaoglu, 2011; Lee, 2010; Moldovan, 2011).

During anodization of Al, AAO is formed as a result of oxidation reactions which will be discussed later. Unlike the rest of the surface treatments such as electroplating, anodizing takes place on the interchange surface between aluminium and aluminium oxide, this grows inwards aluminium.

Aluminium is a unique metal among the rest of the metals those can be anodized, (e.g. niobium, tantalum, titanium, tungsten) since either a thick non-porous oxide or a coating consisting of pores in nano-scale can be achieved by anodizing. The anodic alumina oxide (AAO) structure, which has nano pores thus also named as nanoporous anodic alumina (NPAA)

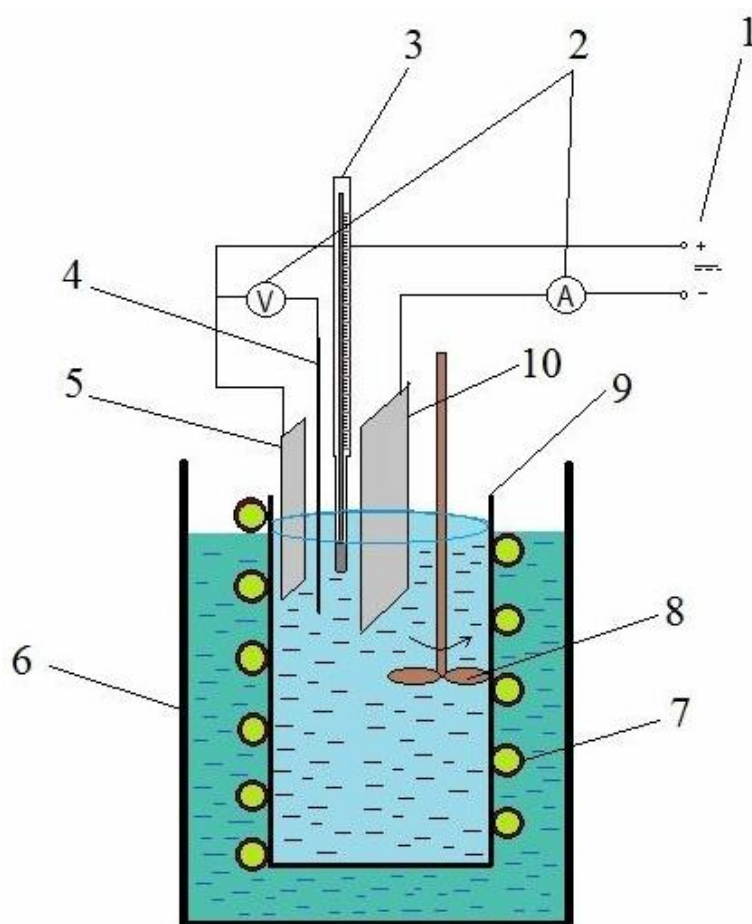
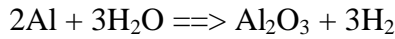


Figure 2.3: Schematic representation of the experimental setup (Moldovan, 2011).

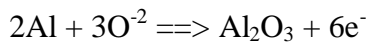
There are two different oxide types can be grown on aluminium depending on the electrolyte used during anodization. Nonporous (barrier) oxide film grows in solutions that alumina has very low solubility, such as solutions containing borate, phosphate or tartrate compounds. pH of the electrolyte should be between 5 and 7 for such a formation. In case of using an electrolyte in which aluminium oxide has limited solubility, porous oxide film can be obtained with simultaneous formation-dissolution reactions. Dilute sulphuric, oxalic or phosphoric acids can be used for such oxide film production (Hagelsieb, 2007; Choi, 2004). In this study, we will be mainly focused on porous type AAO.

Anodization is an electro-chemical process and during the anodization there occur reactions between anode, cathode and electrolyte. In a typical anodizing process, an aluminum plate is connected to the anode of a DC source. A weak acid solution is used as electrolyte. The cathode can be made from any conductive material that is chemically inert in the electrolyte used. When applying potential, hydrogen ions are

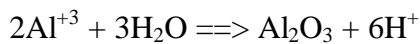
reduced in order to form hydrogen gas at the cathode and aluminum is oxidized into Al^{+3} cations. Some of these cations are dissolved in the electrolyte, and a part forms an oxidic layer on the metal surface. For further reaction, oxygen-containing anions are supplied by the electrolyte (Moldovan, 2011). The main reactions of anodization is;



This is the sum of the separate reactions at each electrode. The reactions at the anode occur at the metal/oxide and oxide/ electrolyte interfaces. The ions that make up the oxide are mobile under the high field conditions. At the metal/oxide interface the inward moving oxygen anions react with the metal:



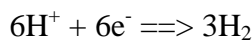
At the oxide/electrolyte interface outward moving aluminum cations react with water:



(In case of aluminum dissolution into the electrolyte during porous film formation, the anodic reaction is:



The reaction at the cathode is hydrogen gas evolution:



The so formed AAO can be sealed to increase its corrosion resistance by plugging the pores. Sealing is generally conducted in hot water.

The sealing reaction can be written as:



2.2 Two-Step Anodization

In 1995, Masuda and Fukuda discovered that anodic alumina oxide could exhibit self-ordered porous structure in case of anodizing for long durations in 0.3M oxalic acid. They reported that the pores arranged regularly formed a honeycomb structure. After this breakthrough point of AAO fabrication, many scientists began working on AAO and this effort ended up with the development of two-step anodization process.

Two-step anodization provided production of AAO with highly ordered nano-pores. Thus, anodization of aluminium became a greater point of interest especially for those who are working in nanotechnology field (Masuda,1995; Choi, 2004; Lee, 2010).

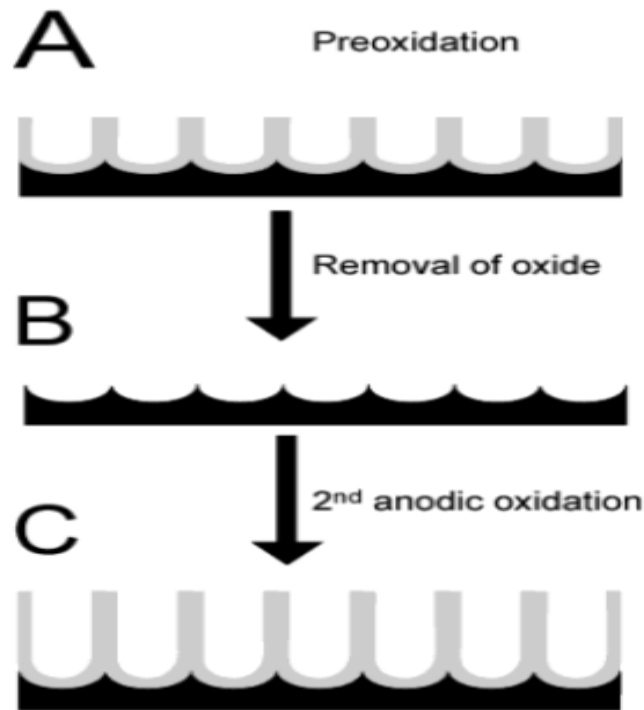


Figure 2.4: Two step anodization steps a) Electropolished surface, b) First anodization, c) Oxide removal, d) Second anodization (Yuan, 2004).

Porous structure starts to form in the first anodization step; however, the pore structure that is obtained from first step anodization is not in the ordered form (Fig. 2.4). Pores start to grow inwards aluminium base in random directions until all the tube bottoms are at the same level, parallel to each other and first anodization process ends up with this structure. After the first anodization step, oxide layer should be etched in order to grow highly ordered porous structure with a second anodization step. By removing this oxide, a pre-pattern is produced on aluminium (Fig. 2.4). Finally a second anodization, which is basically the same as the first one, is performed to produce a surface consisting of well-ordered nano pores (Fig. 2.5 and Fig. 2.6) (Zhao, 2007; Sulka, 2006; Lee, 2011; Choi, 2004; Ko et al., 2006).

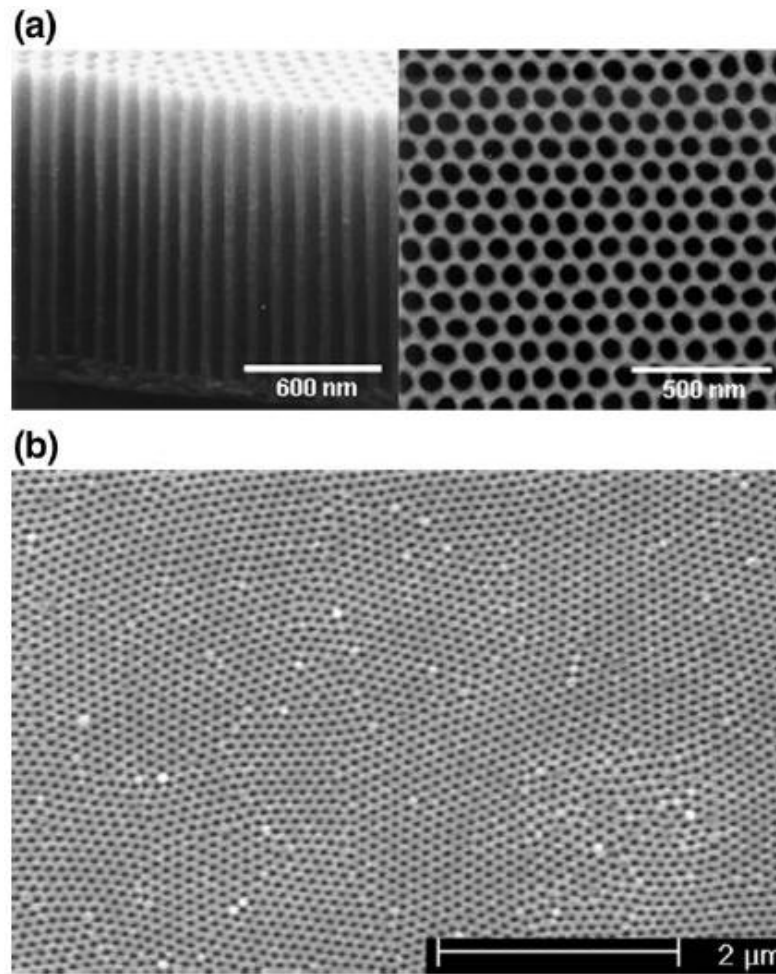


Figure 2.5: FEG-SEM image of two-step anodized AAO structure with 30 nm pore diameter obtained in 0.3 M oxalic acid solution with 15 °C and 40 V: (a) side and top view, (b) macroscopic distribution of pores in a random fashion (Ko et al., 2006).

Masuda and Fukuda performed two-step anodization in 0.3M oxalic acid bath first time. Since then, as mentioned previously, two-step anodization became a point of interest. There are many different electrolyte for using anodization process and each electrolyte has own voltage and temperature properties. As an example; Sulphuric acid is suitable for potentials between 5 ~40V while oxalic acid can be used within a range of 30 -120V and phosphoric acid is capable of handling potentials varying between 80 -200V.

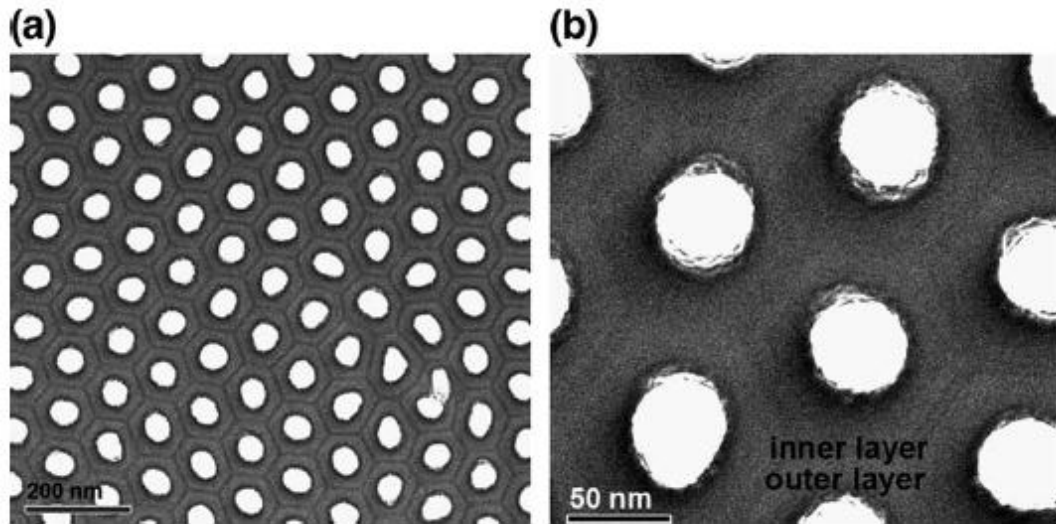


Figure 2.6: STEM image of AAO structure: (a) AAO structure after the second anodization step (no widening; diameter: about 30 nm); (b) an enlarged image of (a); (Ko et al., 2006).

Many research groups proved the relation of voltage with AAO layer thickness. Figure 2.7 shows influence of voltage upon AAO layer thickness within time. It is clear that increase in voltage end up with increase in AAO layer thickness.

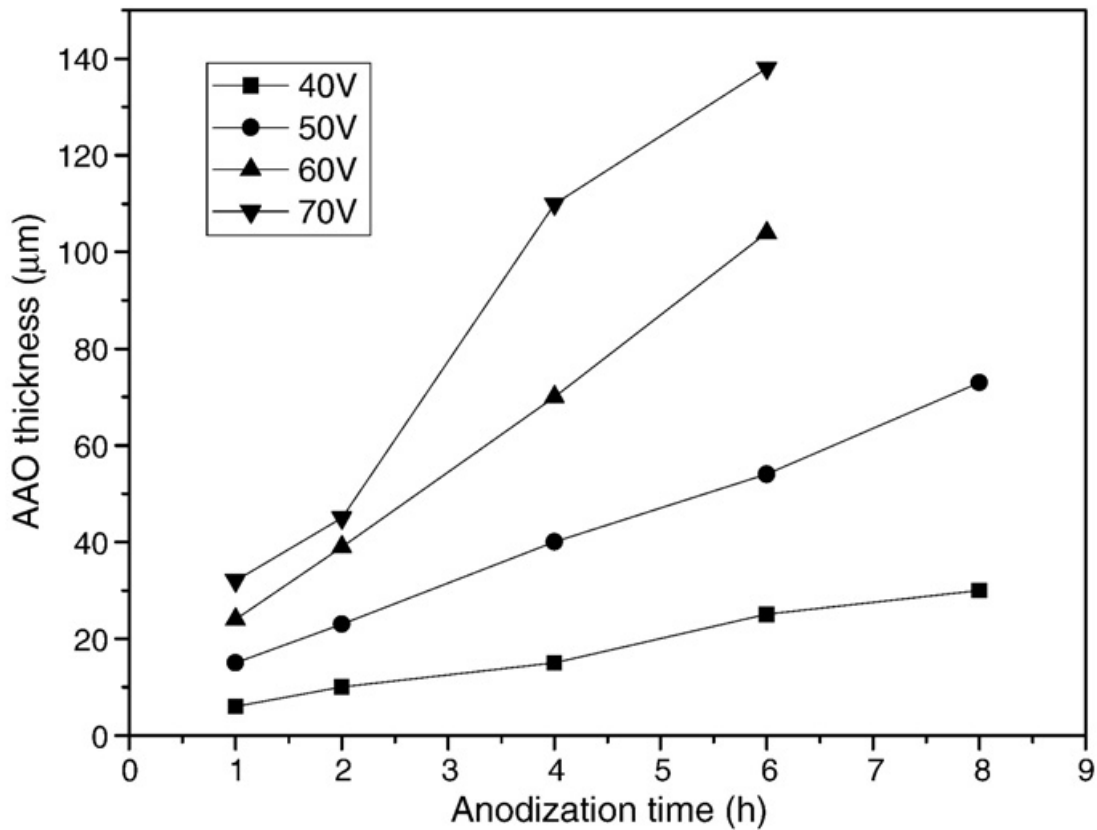


Figure 2.7: Influence of voltage upon AAO layer thickness (Patermarakis, 2007)

Many scientists used different electrolyte according to the porous structure required. Lee and colleagues used both oxalic acid and phosphoric acid for the production of AAO with various pore diameters. Sulka performed two-step anodization in sulphuric acid (20% wt) at low temperatures ($\sim 1^{\circ}\text{C}$) at potentials between 15 and 25V. It should be noted that each type of bath used has its own potential range. Zhao was one of the researchers who also preferred sulphuric acid bath. Working temperature of the first step anodization varied between 0 and 30°C . (Masuda, 1995; Zhao, 2007; Sulka, 2006; Lee, 2011; Choi, 2004).

Table 2.1 shows electrolyte types these used in anodization process for obtaining nanoporous structure.

Table 2.1: Major acid components of typical electrolyte types used to produce porous oxide layer on an aluminum substrate (Poinern, 2011).

Main Acid used in Electrolyte	Molecular Formula	Concentration (M)	Pore Size Range (nm)
Acetic	$\text{CH}_3\text{CO}_2\text{H}$	1	Not specified
Citric	$\text{HO}_2\text{CCH}_2(\text{OH})(\text{CO}_2\text{H})\text{CH}_2\text{CO}_2\text{H}$	0.1 to 2	90 to 250
Chromic	H_2CrO_4	0.3, 0.44	17 to 100
Glycolic	$\text{CH}_2(\text{OH})\text{CO}_2\text{H}$	1.3	35
Malic	$\text{HO}_2\text{CH}_2\text{CH}(\text{OH})\text{CO}_2\text{H}$	0.15 to 0.3	Not specified
Malonic	$\text{CH}_2(\text{CO}_2\text{H})_2$	0.1 to 5	Not specified
Oxalic	$\text{C}_2\text{H}_2\text{O}_4$	0.2 to 0.5	20 to 80
Phosphoric	H_3PO_4	0.04 to 1.1	30 to 235
Sulfuric	H_2SO_4	0.18 to 2.5	12 to 100
Tartaric	$\text{HO}_2\text{CCH}(\text{OH})\text{CH}(\text{OH})\text{CO}_2\text{H}$	0.1 to 3	Not specified

In anodization process there are many different parameters such as electrolyte type, concentration of electrolyte, temperature, voltage, stirring speed, these have effect on properties of NPAA, such as pore diameter, interpore distance, wall thickness, membrane thickness.

2.2.1 Pore diameter

Pore Diameter is one of the important parameter in NPAA membrane fabrication, because pore diameter has direct influence on NPAA membrane applications, such as nanowire and nanorod fabrication. One of the most important application areas of NPAA membranes is nanostructure fabrication. For nanostructures, sizes of pores are very important, because it affects the electrical and magnetic properties of the

material. Since of NPAA membranes have very wide adjustable properties, many scientist worked on the optimization of the NPAA membrane fabrication process.

Because the pore diameter determines radius of the obtained nanostructures that is planned to be used as NPAA template for fabrication, it is an important parameter. Generally, for the anodic porous alumina structure, the pore diameter is linearly proportional to the anodizing potential multiplied with proportionality constant λ_p (approximately 1.29nmV^{-1}) where D_p is a pore diameter (nm) and U denotes the anodizing potential (V) (2.1);

$$D_p = \lambda_p \times U \quad (2.1)$$

Fig.2.8 shows the anodization parameters these have influence on pore diameter (O’Sullivan, 1970).

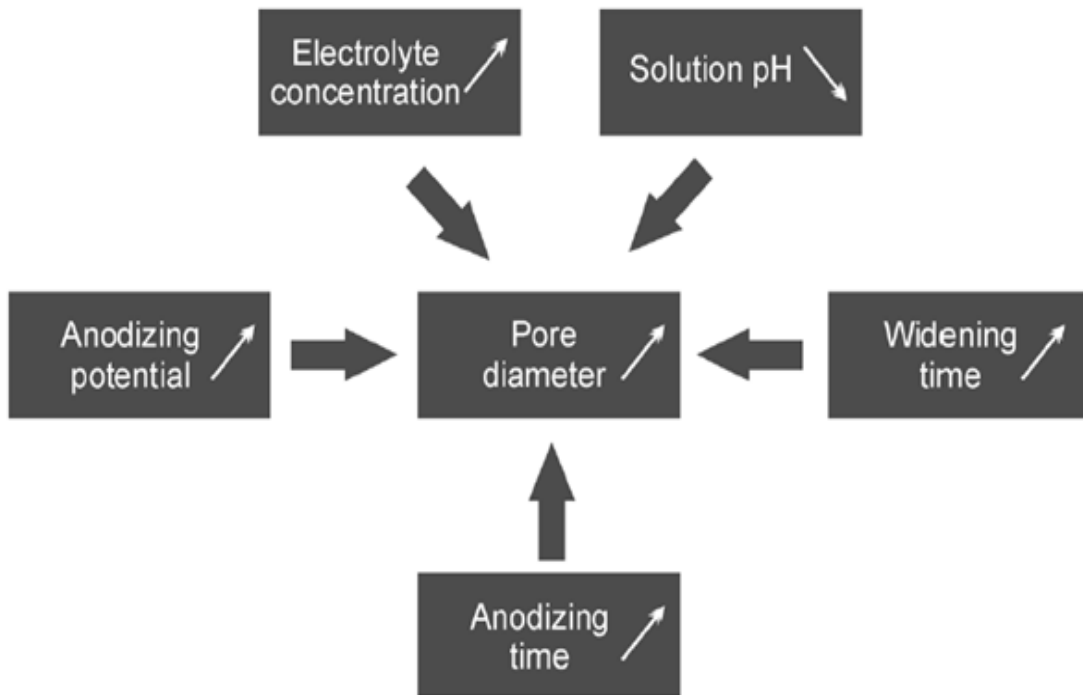


Figure 2.8: Parameters these have influence on pore diameter (Sulka, 2008)

According to Fig. 2.8, increasing in anodizing potential and time, electrolyte concentration and widening time, increase pore diameter and increasing in solution pH, decrease pore diameter.

Other two parameters that effect on the pore diameter are electrolyte temperature and stirring speed of electrolyte. Pore diameter increase with increasing temperature and decrease with increasing stirring speed.

The dependence of the diameter on the voltage is not sensitive to the electrolyte. The literature about NPAA membranes generally examines areas; near top surface or pore bottoms. Anodizing time has a little effect on the diameter of pores in the inner oxide (Keller, 1953; Thompson, 1997).

The reason of a higher diameter of pores observed in a region close to the film surface is irregular initial growth of the pores during the very early stages of pore development, and their further reorganization in a hexagonal arrangement. It should be noted that an enhanced chemical dissolution of oxide, resulting in the development of widened pores, might occur also during anodizing at a sufficiently high temperature, or in strong acidic solutions (Thompson, 1983; 1997).

The acidic electrolyte etch along the cell walls, and especially in the outer oxide layer, increases the diameter of pores measured at the surface of the anodic film (Wood, 1968).

According to early studies about nanoporous anodic alumina, scientist belived that pore diameter was independent of the forming potential (Keller, 1953). However, later studies have reported anodizing potential or current density have influence upon the pore diameter as a parameter (Paolini, 1965).

The pore diameter for anodizations conducted at a constant anodizing potential can be calculated as follows (2.2):

$$D_p = D_c - 2 \times W = D_c - 1.42 \times B = D_c - 2 \times W_U \times U \quad (2.2)$$

where D_c is the cell diameter, interpore distance (nm), W is the wall thickness (nm), B is the barrier layer thickness (nm), and W_U is the wall thickness per volt (nm/V) (O'Sullivan, 1970).

For potentiostatic conditions of anodization, wall thickness divided by the anodizing voltage gives the thickness of oxide-wall per applied volt (W_U). The empirical dependence of pore diameter on the anodizing potential or the ratio of anodizing potential to a critical value of the potential (U_{max}) has been reported by Palibroda (Palibroda, 1984) (2.3):

$$D_p = 4.986 + 0.709 \times U = 3.64 + 18.89 \times U / U_{\max} \quad (2.3)$$

Obviously, the temperature of the electrolyte and the stirring speed of electrolyte in the electrolytic cell affect the pore diameter. Figure 2.9 shows the effect of electrolyte temperature on anodization.

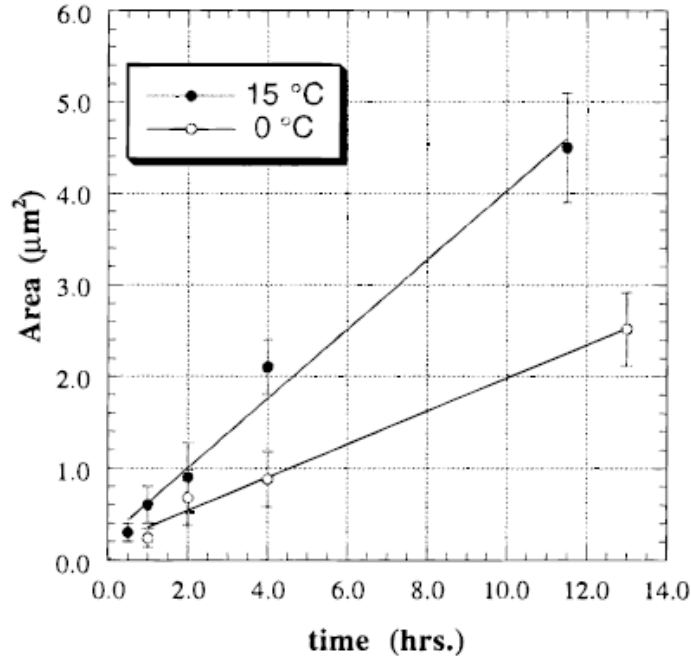


Figure 2.9: Effect of electrolyte temperature on anodization (Li, 1998)

At higher temperatures of anodizing (e.g., near room temperature) a significant acceleration of chemical dissolution of the outer oxide layer, especially in a strong acidic solution is expected. On the other hand, low stirring speed of the electrolyte during anodizing under the constant anodizing potential causes a significant increase in the local temperature at the inner oxide layer, and the recorded current density increases (Li, 1998). As a result of the increasing local temperature, a chemical dissolution of oxide in the inner layer, as well as the electrochemical formation of anodic oxide layer, are accelerated. The effect of electrolyte stirring on a pore diameter is shown schematically in Figure 2.10.

The datas from experiments show that electrolyte temperature and electrolyte concentration have influence upon pore diameter. For instance, the pore diameter has been found to depend on temperature for the constant potential anodizing in a phosphoric acid solution (O'Sullivan). With increasing the temperature of the electrolyte, an increase in pore diameter in the outer oxide layer has been noted. At

the same time, a decrease in pore diameter in the inner oxide layer has been observed.

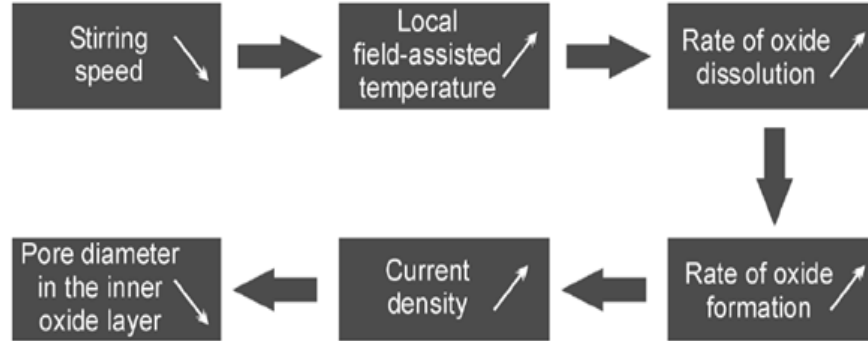


Figure 2.10: Effect of stirring on the pore diameter of nanostructures obtained by anodization of aluminum (Sulka, 2008)

According to O’Sullivan and Wood, electrolyte concentration does not significantly influence the pore diameter (O’Sullivan, 1970). On the other hand, studies that are more recent suggested that the pore diameter decreases with decreasing pH of the solution (Parkhutik, 1992) and temperature (Sulka, 2007). A decrease in pore diameter with increasing concentration of the acidic electrolyte can be attributed to decreasing pH.

The other parameter about pore shape is its formation. Nanoporous structures form by force of self-ordering and pores are forming in a hexagonal shape. In a number of studies the geometry of hexagonal formation are investigated.. Sui reported the differences in the geometry of AAO that are obtained in two different electrolytes; oxalic acid and sulfuric acid (Sui, 2001).

A summary of the influence of anodizing parameters on the pore diameter of a nanostructure formed under potentiostatic conditions is presented schematically in Figure 2.8. Therefore, a significant variation in pore diameter determined for similar anodizing conditions and electrolytes is reported in the literature.

Interpore distance is another important parameter for NPAA. Interpore distance is the sum of pore radius and wall thickness (W). However, the parameters affecting pore radius and wall thickness are not the same, so we should examine interpore distance separately from these parameters.

Table 2.2: Geometric parameters of the hexagonal pore array (Sui, 2001)

Sample	Hexagonal array percentage	Averaged angle value	Averaged hexagonal area (μm^2)	Pore density (pores/ cm^2)
Sulfuric acid anodized	≈ 66	$120.1 \pm 9.7^\circ$	0.012	2.6×10^{10}
Oxalic acid anodized	≈ 100	$120.0 \pm 5.6^\circ$	0.024	1.2×10^{10}

2.2.2 Interpore distance

It is commonly accepted that the interpore distance (D_c) of anodic porous alumina is linearly proportional to the forming potential of the growth of anodic porous alumina with a proportionality constant λ_c of approximately 2.5nm V^{-1} (Nielsch, 2002) (2.4):

$$D_c = \lambda_c \times U \quad (2.4)$$

According to Keller et al., the cell diameter can be calculated precisely from the following equation (2.5):

$$D_c = 2 \times W + D_p = 2W_U \times U + D_p \quad (2.5)$$

Experiments from O'Sullivan and Wood show that the wall thickness is about 71% of the barrier layer thickness (B) (O'Sullivan, 1970). Taking into account this fact, the following expression can be proposed (2.6):

$$D_c = 1.42 \times B + D_p \quad (2.6)$$

Hwang showed the dependence of anodizing potential on interpore distance (Hwang, 2002). For anodization in oxalic acid conducted under anodizing potential ranges between 20 and 60 V, a linear relation existed between anodization potential (U) and interpore distance (D_c) (2.7):

$$D_c = -5.2 + 2.75 \times U \quad (2.7)$$

Some reaches point out that anodization temperature has little or no effect on interpore distance at the constant (O'Sullivan, 1970). Hwang reported that for oxalic acid anodization process, electrolyte temperature the interpore diameter is independent for interpore distance (Hwang, 2002). Contrary to this, for self-organized anodizing in sulfuric acid, an influence of temperature on interpore distance has been observed (Sulka, 2007).

O'Sullivan and Wood showed that increasing the concentration of electrolyte decreases the interpore distance. In the case when anodizing is carried out in phosphoric acid at constant current density, increasing the temperature of anodizing as well as increasing the electrolyte concentration causes a decrease in the interpore distance in nanostructures (O'Sullivan, 1970).

2.2.3 Wall thickness

There are several studies in the literature on the calculation of wall thickness (W). Sulka reported following equation (2.8):

$$W = (D_c - D_p) / 2 \quad (2.8)$$

According to Sullivan and Wood, the wall thickness built during anodizing in phosphoric acid is related to the barrier layer thickness (B) as follows (O'Sullivan, 1970) (2.9):

$$W = 0.71 \times B \quad (2.9)$$

According to another study that report the relationship between wall thickness and barrier layer in oxalic acid anodization the proportionality between wall (W) and barrier layer thickness (B) varies slightly with anodizing potential in the range of 5 to 40 V. For anodizing potentials between 5 and 20 V, a relationship between W and B with a proportionality constant of about 0.66 has been observed, while for higher anodizing potential a gradual increase in the proportionality constant to the final value of about 0.89 has been reported (Ebihara, 1983).

2.2.4 Barrier layer thickness

Barrier layer is general oxide layer of aluminium metal. If oxidation process occurs in acidic solution, oxide layer is obtained as porous structure. In this situation barrier layer occurs in bottom region of tubes. This is a very thin, dense and compact dielectric layer. The barrier layer has the same nature as an oxide film formed naturally in the atmosphere, and allows the passage of current only due to existing faults in its structure. The existing compact barrier layer at the pore bottoms makes the electrochemical deposition of metals into pores almost impossible. Because of this limit, the thickness of the barrier layer is extremely important and can determine any further applications of nanostructures formed by the anodization of aluminum.

There is directly relation with the thickness of the barrier layer the anodizing potential. Wernick reported the dependence of the thickness of the barrier layer upon the anodizing potential about $1.3\text{--}1.4\text{nmV}^{-1}$ for barrier-type coatings, and 1.15nmV^{-1} for porous structures (Wernick, 1987).

Some variations have been reported in the barrier layer thickness with anodizing potential or the concentration of electrolyte. Evidence of experimental values of B_u , known as an anodizing ratio and defined as a ratio between the thickness of the barrier layer and anodizing potential, are listed in Table 2.2 for a variety of electrolytes (Sulka, 2008).

O'Sullivan reported that variation of the barrier layer thickness per volt depends on whether oxide films are formed at a constant potential or at constant current density regimes (O'Sullivan, 1970).

Moreover, the increase in anodization temperature decreases the thickness of the barrier layer for anodizing at the constant potential. The increasing thickness of the barrier layer with increasing electrolyte concentration suggests that ionic conduction becomes easier under the set current density. Therefore, most of the ionic current passes through microcrystallites in the barrier layer. On the other hand, the observed decrease in barrier layer thickness with increasing electrolyte concentration and anodizing temperature is a direct result of an enhanced field-assisted dissolution of oxide at the oxide/electrolyte interface (Sulka, 2008).

Chu et al. reported the effect of anodizing potential on the thickness of the barrier layer for the anodic porous alumina formed in various electrolytes (It is shown in Figure 2.11). These results suggest a general constant relationship between the anodizing ratio and anodizing potential (Chu, 2006).

For optimum self-ordering conditions (10% porosity of the nanostructure and perfect hexagonal arrangement of nanopores) of anodizing, Nielsch et al suggested that, the barrier layer thickness should be proportional to the interpore distance as follows **(2.10)**:

$$B \approx D_c / 2 \text{ (Nielsch, 2002)} \quad \textbf{(2.10)}$$

$$B \approx D_c / 2 \text{ (Nielsch, 2002)}$$

Table 2.3: Anodizing ratio (B_U) for various anodizing electrolytes (Sulka, 2008).

Electrolyte	Current density ^a (mA cm ⁻²) or anodizing potential ^b (V)	Concentration (M)	Temperature (°C)	B_U (nm V ⁻¹)
H ₃ PO ₄	100 ^a ; 80 ^b	0.4 (3.8%)	20	0.89 ^a ; 1.14 ^b
			25	0.90 ^a ; 1.09 ^b
			30	1.05 ^a ; 1.04 ^b
		1.5 (13%)	25	1.10 ^a ; 1.04 ^b
		2.5 (21%)		1.17 ^a ; 0.82 ^b
	(20–60) ^b	0.42 (4%)	24	1.19 ^b
	87 ^b		25	0.99 ^b
	103 ^b			0.96 ^b
	117.5 ^b			1.08 ^b
	87 ^b	1.70 (15%)		0.99 ^b
	87 ^b	3.10 (25%)		0.97 ^b
H ₂ C ₂ O ₄	(20–60) ^b	0.22 (2%)	24	1.18 ^b
	3 ^b	0.45 (4%)	30	1.66 ^b
	10 ^b			1.40 ^b
	20 ^b			1.19 ^b
	30 ^b			1.10 ^b
	40 ^b			1.06 ^b
H ₂ SO ₄	15 ^b	1.70 (15%)	10	1.00
		1.10 (10%)	21	1.00 ^b
		1.70 (15%)		0.95 ^b
		5.6–9.4 (40–60%)		0.80 ^b
		12.8 (75%)		0.95 ^b
		16.5 (90%)		0.10 ^b
	3 ^b	2.0 (17%)	20	1.45 ^b
	10 ^b			1.23 ^b
	15 ^b			1.05 ^b
	18 ^b			0.92 ^b
H ₂ CrO ₄	(20–60) ^b	0.26 (3%)	38	1.25 ^b
Na ₂ B ₄ O ₇	60 ^b	0.25 (pH = 9.2)	60	1.3 ^b
(NH ₄) ₂ C ₄ H ₄ O ₆	(25–100) ^b	0.17 (3%, pH = 7.0)	–	1.26 ^b
Citric acid	(260–450) ^b	0.125	21	1.1 ^b

^aConstant current density anodizing.^bConstant potential anodizing.

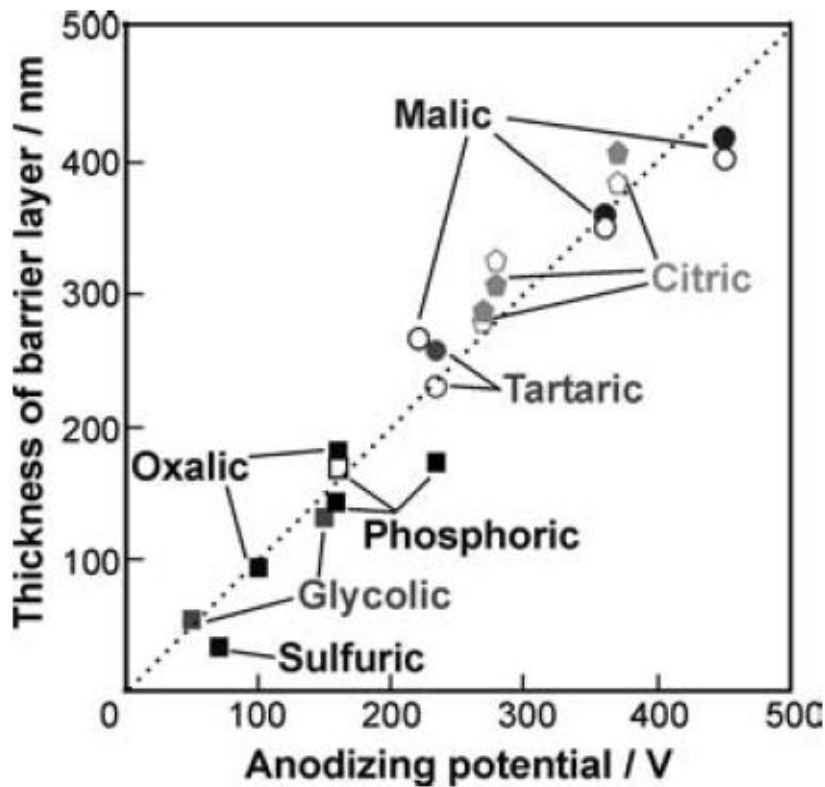


Figure 2.11: Anodizing potential influence on the barrier layer thickness for anodic porous alumina formed in sulfuric, oxalic, glycolic, phosphoric, tartaric, malic, and citric acid solutions (Chu, 2006).

The wall thickness, as well as the barrier layer thickness, in nanostructures formed by anodization can be easily altered by post-treatment procedures involving chemical etching; this is known as a process of isotropic pore widening.

2.2.5 Oxide removal

Oxide removal process is important to obtain highly ordered nanoporous membranes. After etching the oxide only pore bottoms left and they are using for pre-pattern for oxidation. Therefore, in the second oxidation, pore structure grows more orderly. Oxide removal is generally performed by immersing first-step anodized samples in a chromic acid- phosphoric acid solution consisting of 6 wt. % phosphoric acid, 1.8 wt. % chromic acid at 60-80°C. Removal time is related with oxide layer thicknesses, also thicker films requires more time for etching.

Zaraska performed oxide removal process for durations varying from 10 minutes to 15 minutes for samples that are produced in sulphuric acid. Pasaoglu ran the first step in 0.3M oxalic acid bath and oxide removal was done for 1 hour. (Zaraska, 2010; Pasaoglu, 2011).

Erdogan reported effect of different etching times to oxide removal process. The chemical etching was employed in a mixture of 3.5% H_3PO_4 and 2% CrO_3 (percentages in wt %) at 55°C for 5, 15, 30 and 60 minutes. Erdogan reported that 5 and 15 minutes is not enough to etch all layer that obtained in a solution of 0.6 M $\text{H}_2\text{C}_2\text{O}_4$, at a temperature of 20°C , under 40 V for 30 minutes and etching process has influence upon the pore formation (Erdogan, 2012).

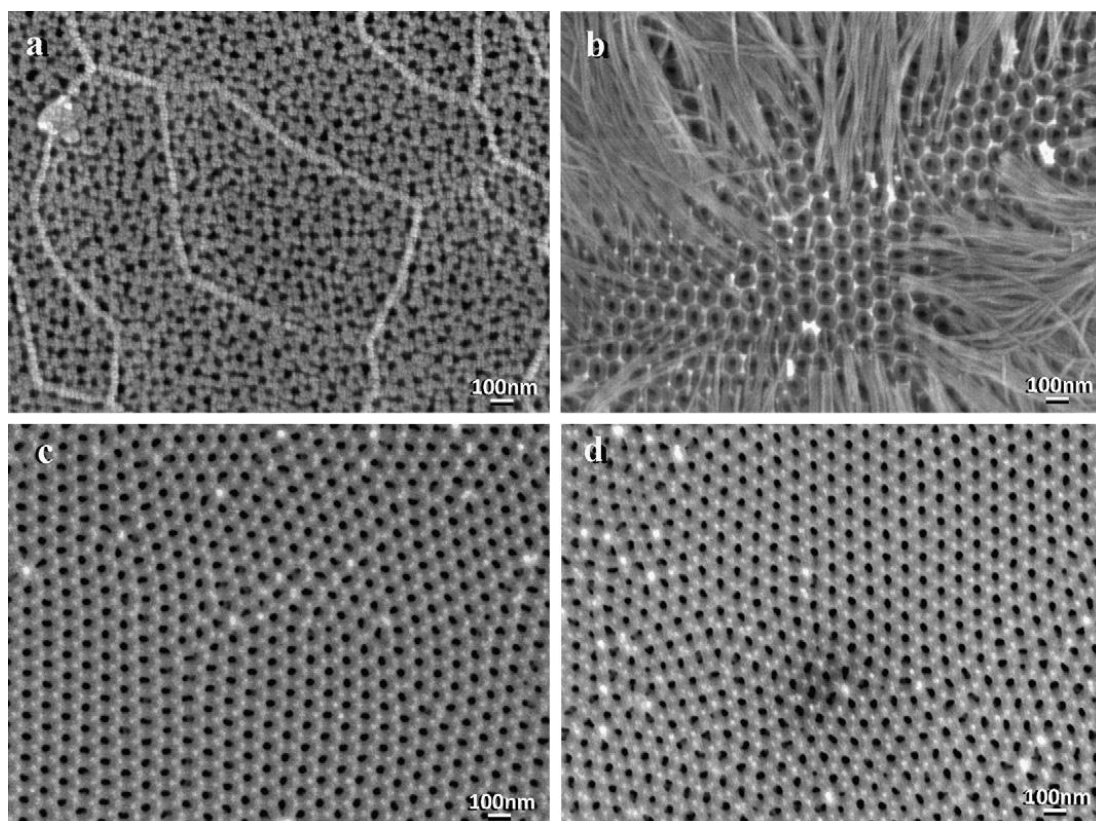


Figure 2.12: Top view FESEM images of AAO templates prepared by using different etching times (a) 5 min (b) 15 min (c) 30 min (d) 60 min (Erdogan, 2012).

2.3 Detachment of NPAA from Aluminium Surface

Detachment of NPAA from aluminium surface was complex problem for the scientist before. Because as mentioned above nanoporous anodic oxide grown on top of aluminium substrate in the anodization process and substrate and oxide layer are connected each other with barrier layer. The most common approach to overcome this problem is to etch away the base aluminum substrate by using heavy metal salts such as HgCl_2 or CuCl_2 . After that, the exposed barrier layer should be dissolve by

using H_3PO_4 dilute aqueous solution, thus opening up the blocked ends of the alumina channels (Xu, 2003). There are some drawbacks of these detachment methods, but this method inevitably lead to pore widening due to partial dissolution of pore walls because of H_3PO_4 . Therefore, there is possible contamination from heavy metal ions too. The main drawback of this process of pore opening in a controlled and reproducible way is the most difficult procedure in obtaining complete through-hole PAA membranes because there are many parameters dependent on the acid strength, dissolution time and type of contact.

In another approach, the anodic oxide film was separated from the aluminum substrate by reversing the polarity of the cell voltage at the final stage of anodization, in which the acid etching process is also necessary to remove the barrier layer (Kyotani).

Xu et al., developed a different approach to detach NPAA. According this method, NPAA structure covering a protective layer after the second anodization, but this method based on chemical etching too (Xu, 2002).

Recently some researches focused to obtain NPAA membrane by alternative ways. Detaching NPAA membrane with short voltage pulse is one of the promising methods. Yuan et al., reported detaching the NPAA membrane from the aluminum substrate by using a short voltage pulse in a high concentrated solution of HClO_4 and butanedione (Yuan, 2004) Figure 2.13 show the schmetic drawing of detachment process with short voltage pulse.

This simple and rapid method is better than those chemical-etching methods, because with this method detachment of alumina from aluminum substrate and dissolution of the barrier layer can be obtained in one simple step. Moreover, the pore size does not change during the process and there is no heavy metal contamination in this method. Consequently, the problems caused by residues of metal ions do not exist. However, this method has some drawbacks too, such as the obtained through-hole NPAA must be subsequentially rinsed by acetone thoroughly in order to remove the viscous butanedione. Therefore, high concentrated solution of HClO_4 and butanedione is not an environmentally friendly option.

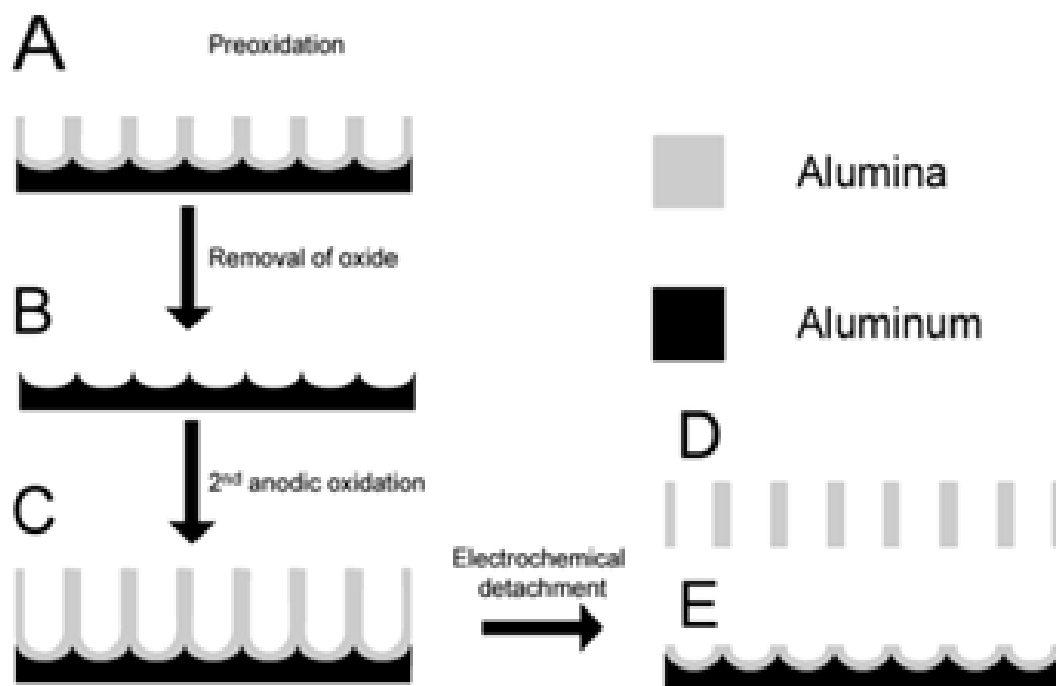


Figure 2.13: Schematic representation of the fabrication procedure for the formation of ordered and through-hole porous alumina membrane. (A) Formation of the porous alumina layer after the first anodic oxidation process; (B) removal of the porous alumina layer; (C) formation of the ordered porous alumina layer after the second anodic oxidation process; (D) free-standing PAA; and (E) the barrier layer structure on aluminum base after electrical detachment of the PAA (Yuan, 2004).

Yuan and his group focused to find alternative detachment solutions and in year 2006, they published a paper about this subject. Their study is on the influence of detachment voltage to detachment process and influence of detachment solutions to detaching results.

To examine influence on short pulse voltages of 0–15 V higher than the film forming potentials on detachment they applied different voltages to the PAA/Al hybrid anodes formed at 30 or 40 V in a 0.3M $\text{H}_2\text{C}_2\text{O}_4$ solution. Figure 2.14 shows their results. They observed that there is no significant anodic current transient, when the pulse voltage was the same as the film forming potential (Fig 2.14, crosses) and detachment of the PAA film failed. On the other hand, when a pulse voltage higher than the film forming potential was applied, a significant peak-like current transient could be observed.

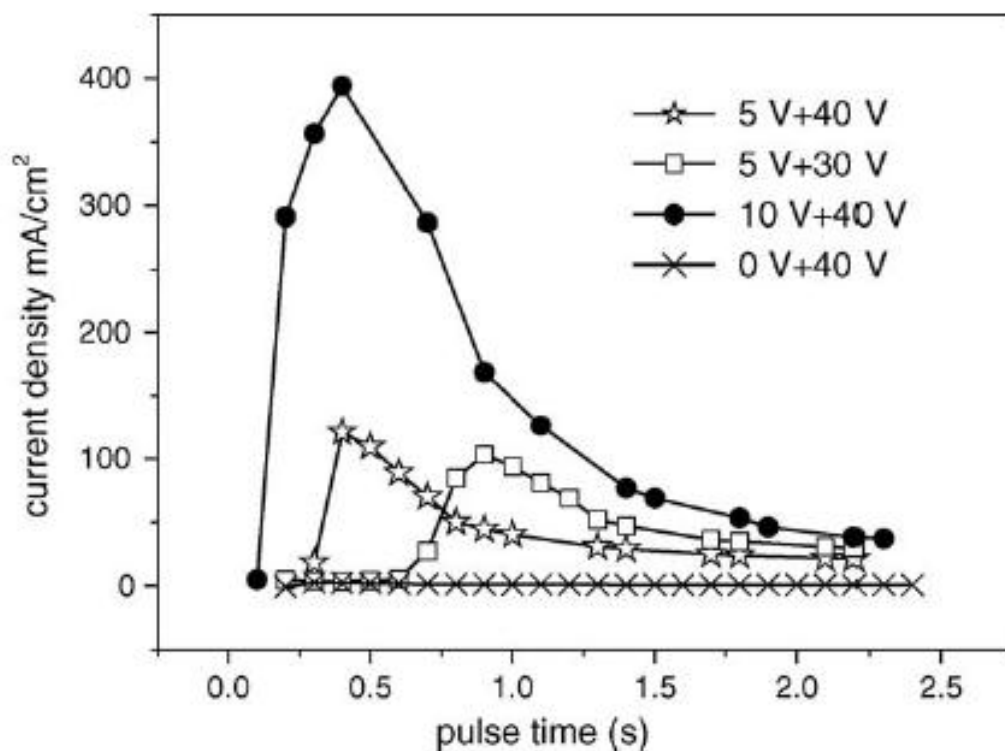


Figure 2.14: Effect of different detaching voltage (*) 5+40V; (□) 5+30V; (●) 10+40V; (×) 0 + 40V on the current density in a solution of 70% HClO_4 + 98% $\text{CH}_3\text{COCOCH}_3$ (v/v = 1:1) at 25 °C for 3 seconds. The PAA film–Al hybrids were formed at different anodic oxidation voltage (40 or 30 V) in a 0.3M $\text{H}_2\text{C}_2\text{O}_4$ solution at 25 °C for 4 hours (Yuan, 2006).

In addition, the peak current increased with the increase of the pulse voltage. For a pulse voltage of 5 V higher than the film forming potential partial detachment of the PAA membrane from the base occurred. Complete detachment of the PAA film could be achieved by increasing the pulse voltage, e.g. 10 V higher than the film forming potential (Figure 2.14, solid circles). For pulse voltage of 15 V higher than the film forming potential, the transient current is too high, leading overload (Yuan, 2006) .

These results demonstrate that pulse voltages of 5–10V higher than the film forming potential should be applied in order to achieve successful detachment of the PAA film and an “optimal” pulse voltage of 10V higher than the film forming potential seems to be appropriate for the detachment of the PAA film from the Al base (Yuan, 2006).

Futhermore, Yuan and his group examine the effect of different detachment electrolytes to the detaching results of NPAA membrane (Table 2.4).

Table 2.4: Detaching results and the corresponding parameters of some electrolytes (Yuan, 2006).

Electrolyte (v/v = 1:1)	Peak current density (mA/cm ²)	Detaching results
HClO ₄ + CH ₃ COCOCH ₃	392	Yes, negligible dissolution
HClO ₄ + (CH ₃ CO) ₂ O	178	Yes, negligible dissolution
HClO ₄ 20 mL + PEG-20000 (4 g/20 mL)	588	Yes, negligible dissolution, but the film is fragile
HClO ₄ + H ₂ O	630	Yes, slight dissolution
HClO ₄ + C ₂ H ₅ OH	416	Yes, slight dissolution
HClO ₄ + TX-10	3	No
HCl (30%)	Overload	Yes, part dissolution and Cl ₂ formation
HNO ₃ (30%)	189	Yes, part dissolution
NaOH (3 M)	13	No
H ₃ PO ₄ (72%) + CH ₃ COCOCH ₃	8	No

The another research group reported a improved way to detach NPAA membrane from aluminium surface by mixture of HClO₄ and ethanol, which is more environmental friendly and efficient as compared to the conventional electrochemical detachment methods. Furthermore, they investigated the influence of the pulse voltage and the nature of the detachment solution on the detaching efficiency (Chen, 2006).

Figure 2.15 shows the SEM images of the surface of detached NPAA membranes. Average pore diameter is 55 nm and it is same with top surface diameter (Figure 2.15a), which suggests that the pulse voltage detachment process has negligible influence on the pore morphology.

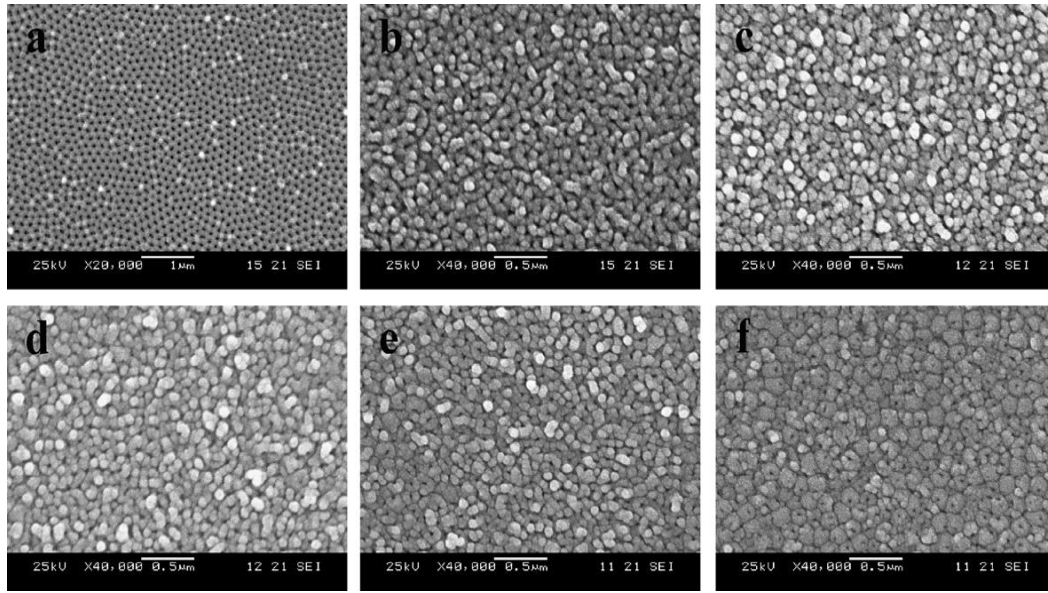


Figure 2.15: SEM images of (a) the surface and (b) the bottom view of the through-hole PAA membrane detached at 70 V for 3 s in 1:1 HClO₄ + ethanol mixture. Bottom images of the PAA membranes detached at (c) 65 V, (d) 62 V, (e) 60 V, (f) 59 V. The PAA was formed at 60 V in a 0.3M oxalic acid and the thickness was 70 μ m (Chen, 2006).

The pores from the bottom surface of PAA could be clearly seen in all the case when the detachment can be successfully accomplished. The pore size of the bottom surface can reach 45 nm when 70 V pulse was applied for the detachment process.

However, the pore size decreases significantly with the pulse voltage (Figure 2.16). When the pulse voltage of 59 V was applied, the barrier layer can be obviously observed although the pores are somewhat open (Chen, 2006).

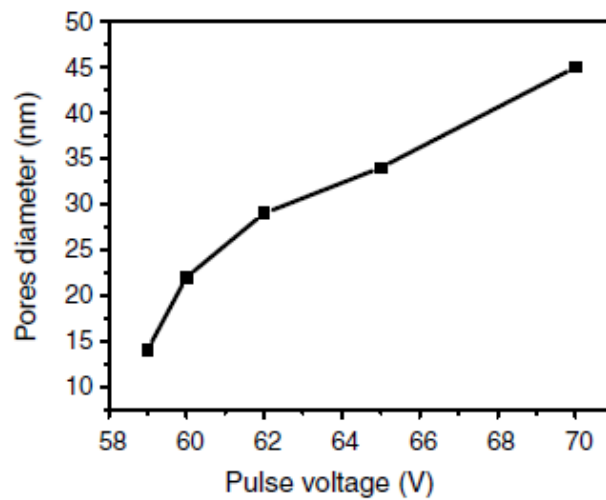


Figure 2.16: Dependence of the open pores diameter on the detaching voltage (Chen, 2006)

3. EXPERIMENTAL STUDIES

In our study, for the investigation of the detachment process in perchloric acid + ethanol mixtures the type and temperature of the anodizing electrolyte is kept constant. The anodization electrolyte is chosen as 0.3 M oxalic acid (most widely used concentration for NPAAO production) and 15 °C as temperature for anodization.

Experiments were carried out according to the scheme given in Fig. 3.1 in order to firstly obtain well-ordered nanoporous AAO and then depachment of NPAA membrane from aluminium surface. Lastly, we realized the characterization by using FEG-SEM.

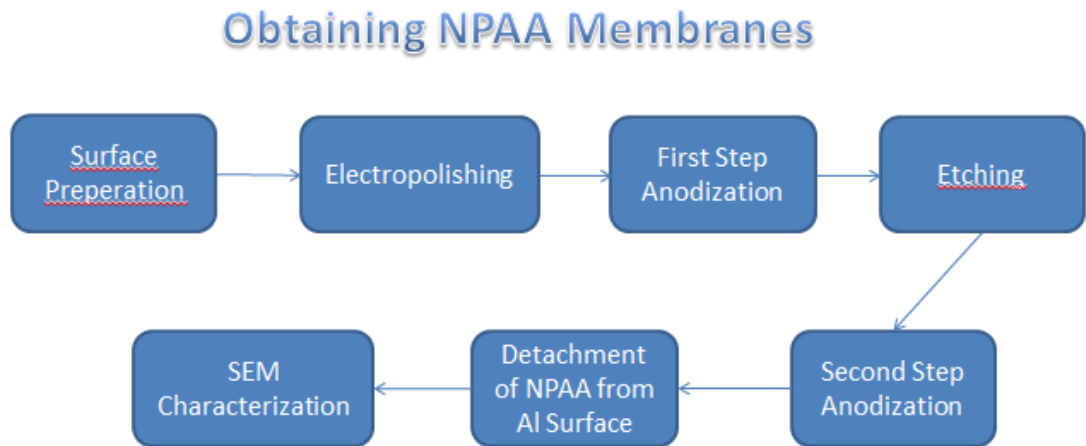


Figure 3.1: Experiment Scheme.

3.1 Experimental Method

Pure aluminium sheets (%99.99) with a thickness of 0.1 mm were cut in the dimensions of 2x4 cm. Samples were then annealed at 400°C for 4 hours for enlarging grain sizes. This annealing process is required for obtaining ordered AAO. Annealed plates were subjected to standard alkaline etching and

desmutting procedure in 10 wt% NaOH solution for five seconds at 55°C for etching and in 10% HNO₃ solution for five minutes at room temperature for desmutting.

3.2 Electropolishing

After annealing and surface cleaning on aluminium samples were electropolished in a commercial (Politoksal EB-35 from Politeknik Metal San. ve Tic. A.S.), Cr free solution based on phosphoric -sulphuric acid mixture which was proposed by Pasaoglu (2011). Electropolishing was conducted for 5 minutes, at a temperature of 55 °C using a potential of 17 V. Electropolishing bath was stirred at a rate of 500 rpm.

3.3 Two-Step Anodization

The anodizing of electropolished samples anodized in oxalic acid electrolyte in order to produce NPAA membranes. We choose oxalic acid bath, because with oxalic acid solution, we are able to obtain NPAA membranes, with a very wide range of morphologic properties. Two-step anodizing was also used in these series of experiments. As electrolyte, 0.3 M oxalic acid was used. Electrolyte temperature was selected as 15 °C for every sample. Parameters such as stirring speed, potential and time were selected differently for every sample according to the Table 3.1. Stainless steel was used as a cathode material during anodization process. After the first anodization, the formed alumina layer was removed by chemical etching in a mixture of 1.8% CrO₃ and 7.1% H₃PO₄ in distilled water at 60 °C for a 1 hour.

3.4 Detachment of NPAA Membrane

After the anodization, NPAA membranes were detached from aluminium surface in a mixture of HClO₄ (70%) and ethanol. Applied voltage was selected according to the anodization voltage of the samples as 10 V in addition to the anodization voltage. 3 seconds voltage pulse is applied to samples and membranes detached from the Al surface after 3 seconds. Stainless steel was used as a cathode material.

Table 3.1: Anodization Parameters.

Numune No	Mixing Speed	Temperauture	1.Step		Etching		2.Step		Detachment
	rpm	°C	Time (hour)	Voltage	°C	Time (hour)	Time (minute)	Voltage	Voltage
1	500	15	1	40	x	x	x	x	x
2	500	15	1	40	60	1	5	40	50
3	500	15	1	50	60	1	5	50	60
4	500	15	1	60	60	1	5	60	70
5	500	15	1	40	60	1	60	40	50
6	500	15	1	40	60	1	120	40	50
7	500	15	1	40	60	1	180	40	50
8	100	15	1	40	60	1	5	40	50
9	900	15	1	40	60	1	5	40	50
20	500	15	1	60	60	1	x	x	x
11	500	15	1	40	60	1	x	x	x
12	500	15	1	60	60	1	60	60	70
13	500	15	1	60	60	1	120	60	70
14	500	15	1	60	60	1	180	60	70
15	500	15	1	50	60	1	60	50	60

4. RESULT AND DISCUSSION

NPAA membranes are characterized by FEG-SEM after the detachment the process. The NPAA properties (film thickness, pore diameter (D_p), interpore distance (D_c), and wall thickness (W), pore bottom morphologies after detachment) determined with SEM are used for:

- Showing the differences in porous structure differences between one-step and two-step anodized surfaces
- Evaluation of these properties with anodization parameters (anodization voltage, stirring speed and time) and comparison of the results with the previous studies.
- Determination of pore bottom morphologies after detachment process for films anodized at different potentials.
- Determination of pore bottom morphology and pore diameter after pore bottom opening process conducted in chromic + phosphoric acid solution.

• The Effect of Two-Step Anodization

To examine the effect of two-step anodization, we compared the surface of one-step anodized sample with the surface of two-step anodized sample (Figure 4.1);

The structure of the two-step anodized surfaces became far more ordered and homogeneous as expected. The pore diameter also increased as a result of second anodization step as explained in section 2.2 (Masuda,1995) Two-step anodization process is used in the rest of the studies.

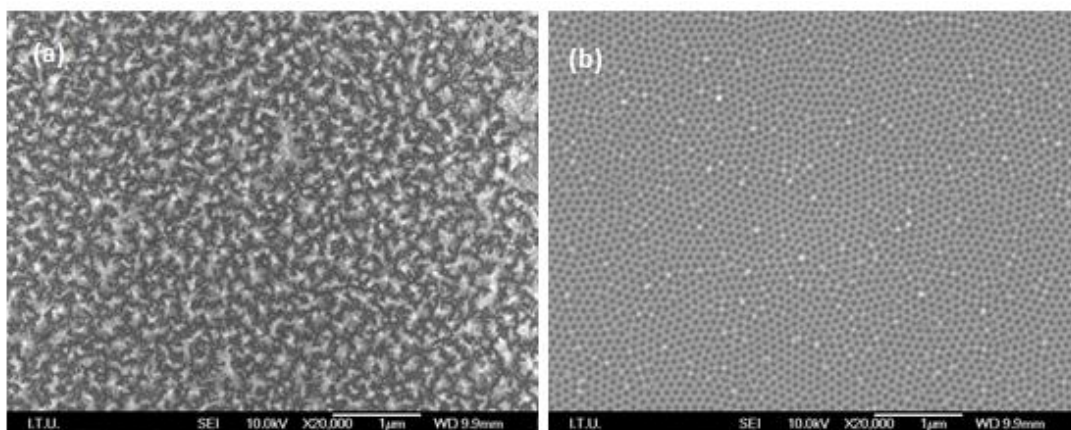


Figure 4.1: (a) FEG-SEM image of NPAA produced with one-step anodization in 0.3 M $C_2H_2O_4$ for 1 hour at 40 V, (b) FEG-SEM image of NPAA after two-step anodization using the same anodization parameters.

- **Influence of Anodization Voltage on the Morphology**

To examine the influence of voltage on the morphology, we produced three two-step anodization samples at three different voltages; 40 V, 50 V and 60 V respectively (Figure 4.2).

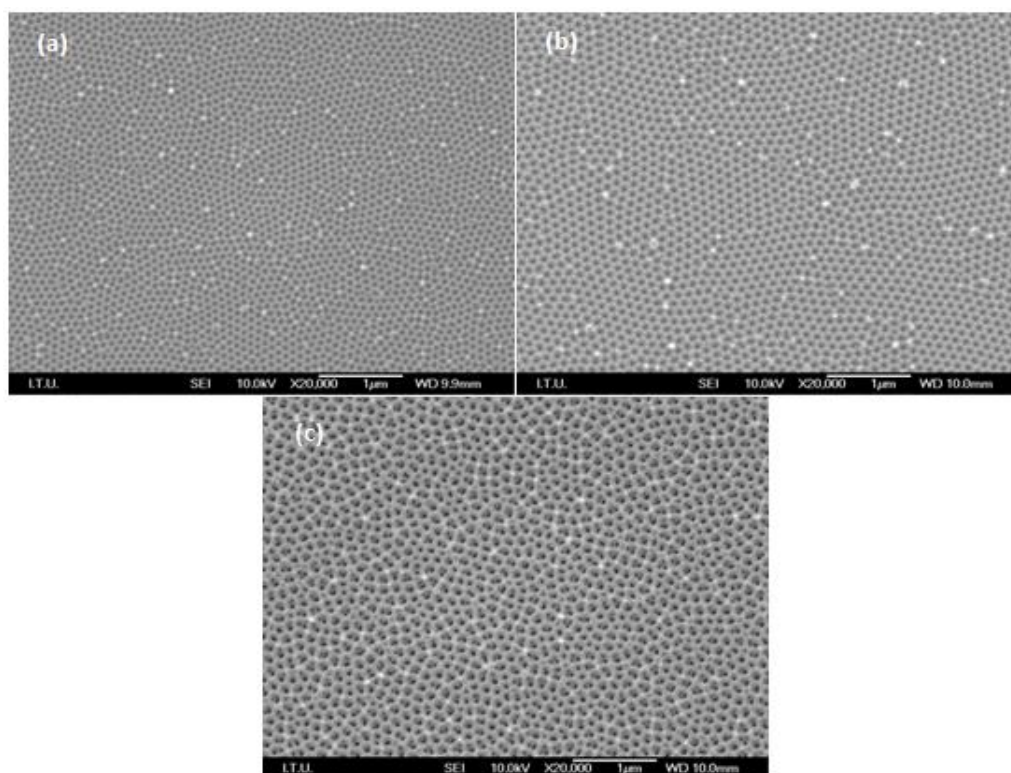


Figure 4.2: FEG-SEM images of NPAA membranes produced by two-step anodization in 0.3 M $C_2H_2O_4$ for 5 min. at (a) 40 V, (b) 50 V, (c) 60 V.

SEM analyses show that by increasing applied voltages, the morphology becomes less homogeneous and pore radius, wall thickness and interpore distances are growing.

- **Influence of Anodization Voltage on the Pore Diameter**

In section 2.2.1, O’Sullivan’s and Paolini’s empirical equations about the relation between voltage and pore diameter are given. Table 4.1 shows the comparison between SEM analysis of this study, O’Sullivan’s and Paolini’s empirical datas;

Table 4.1: Comparison of empirical and therotical datas of pore diameter (nm).

Voltage	Pore Diameter (This Study)	Pore Diameter (O’Sullivan)	Difference (%)	Pore Diameter (Paolini)	Difference (%)
	SEM Analysis	$D_p = \lambda_p \times U$		$D_p = D_c - 2 \times WU \times U$	
40	50,4	51,6	-2,4	42,8	15,0
50	66,2	64,5	2,6	62,1	6,2
60	80,3	77,4	3,6	84	-4,6

According our calculations, there is less difference with O’Sullivan’s equation with our SEM analysis than Paolini’s equation (Figure 4.3).

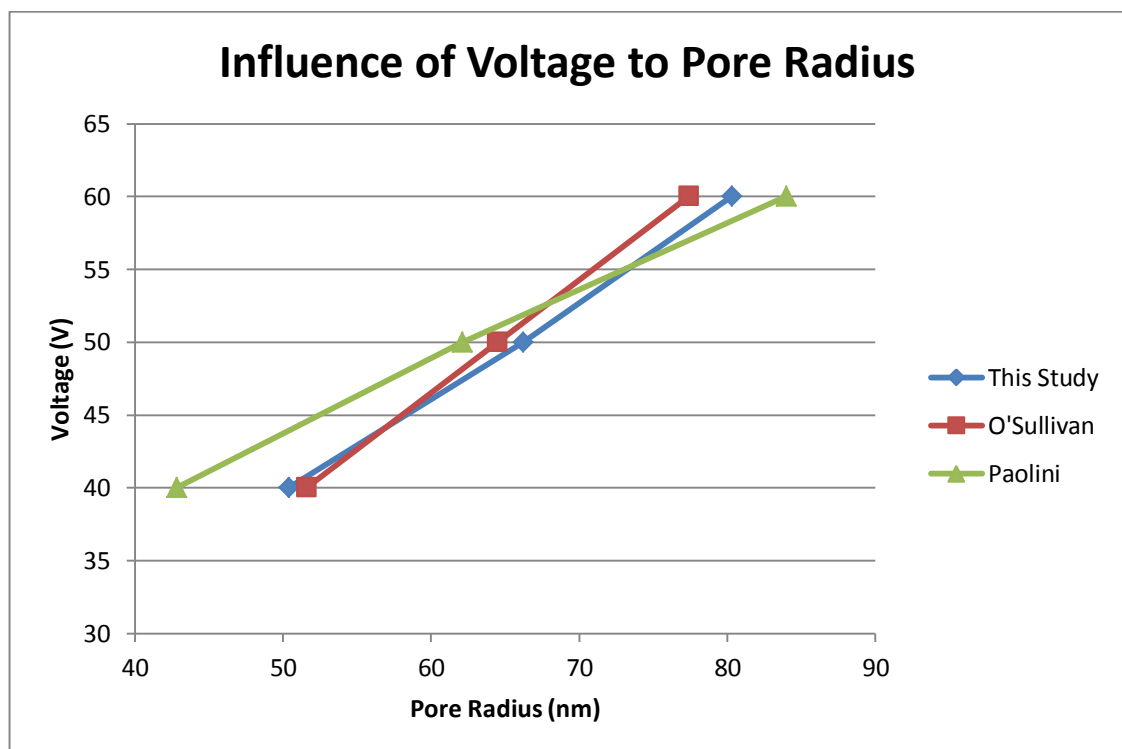


Figure 4.3: Influence of Voltage to Morphology.

- **Influence of Anodization Voltage on the Interpore Distance**

In section 2.2.2, Nielsch's and Hwang's empirical equations about the relation between voltage and interpore distance are given. Table 4.2 shows the comparison between SEM analysis of this study, Nielsch's and Hwang's empirical data;

Table 4.2: Comparison of empirical and theoretical data of interpore distance (nm).

Voltage	Interpore Distance (This Study)	Interpore Distance (Nielsch)	Difference (%)	Interpore Distance (Hwang)	Difference (%)
	SEM Analysis	$D_c = \lambda_c \times U$		$D_c = -5.2 + 2.75 \times U$	
40	103,2	100	3,1	104,8	-1,5
50	128,9	125	3	132,3	-2,6
60	155,2	150	3,3	159,8	-2,9

According our calculations, there is very small difference with both equation. But there is less difference with Hwang's equation with our SEM analysis than Nielsch's equation (Figure 4.4).

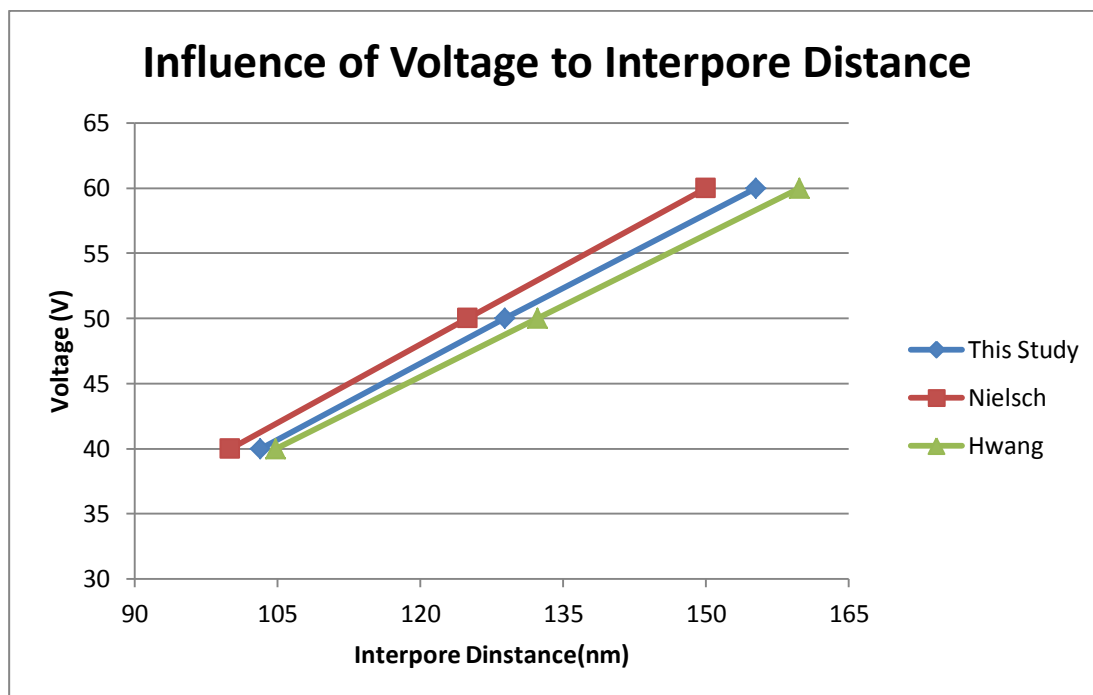


Figure 4.4: Influence of Voltage to Interpore Distance.

- **Influence of Anodization Voltage on the Wall Thickness**

In section 2.2.3, O’Sullivan’s and Sulka’s empirical equations about the relation between voltage and wall thickness are given. Table 4.3 shows the comparison between SEM Analysis of this study, O’Sullivan’s and Sulka’s empirical datas;

Table 4.3: Comparison of empirical and theoretical datas of wall thickness(nm).

Voltage	Wall Thickness (This Study)	Wall Thickness (O’Sullivan)	Difference (%)	Wall Thickness (Sulka)	Difference (%)
	SEM Analysis	$W = 0.71 \times B$		$W = (D_c - D_p) / 2$	
40	30,2	28,4	5,9	26,4	12,6
50	33,4	35,5	-6,3	31,3	6,3
60	35,6	42,6	-19,6	37,4	-5,0

According calculations, our empirical datas are more compatible with Sulka’s equations (Figure 4.5).

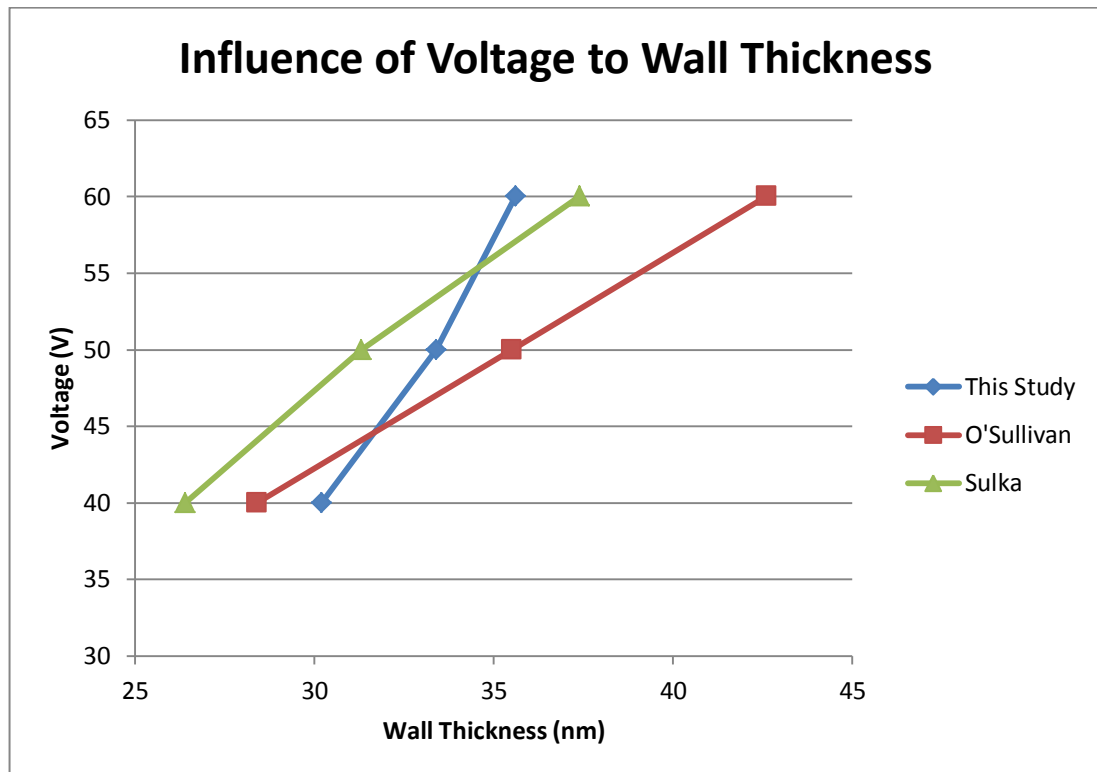


Figure 4.5: Influence of Voltage to Wall Thickness.

- **Influence of Anodization Time on the Membrane Thickness**

To examine the influence of anodization time on the membrane thickness, we produced three two-step anodization samples at three different anodization times; 1 hour, 2 hours and 3 hours (Figure 4.6, Figure 4.7 and Figure 4.8).

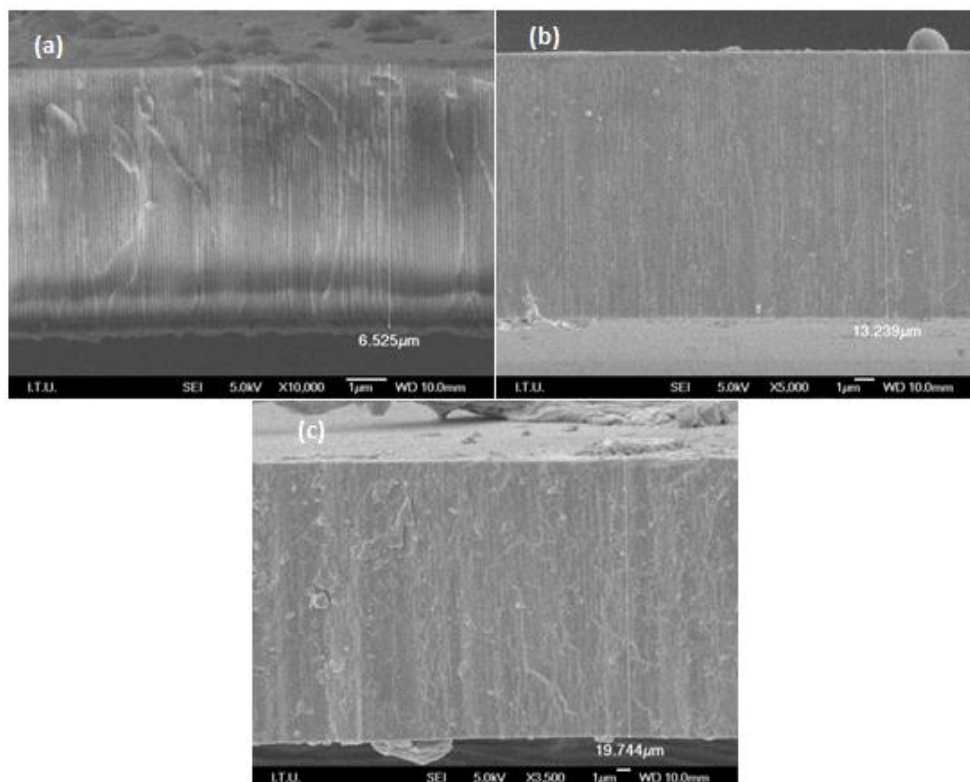


Figure 4.6: FEG-SEM cross-section image of NPAA membrane under the second anodization 0.3 M $C_2H_2O_4$ at 40 V for (a) 1 hour, (b) 2 hours, (c) 3 hours. SEM analysis show that with the increasing in anodization times, membranes become thicker.

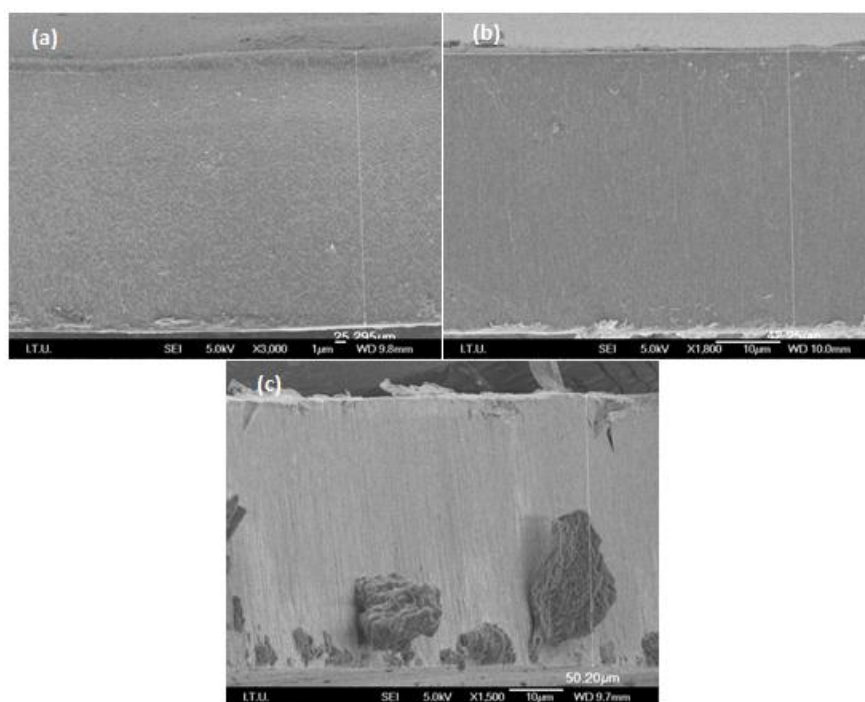


Figure 4.7: FEG-SEM cross-section image of NPAA membrane under the second anodization in 0.3 M $C_2H_2O_4$ at 60 V for (a) 1 hour, (b) 2 hours, (c) 3 hours.

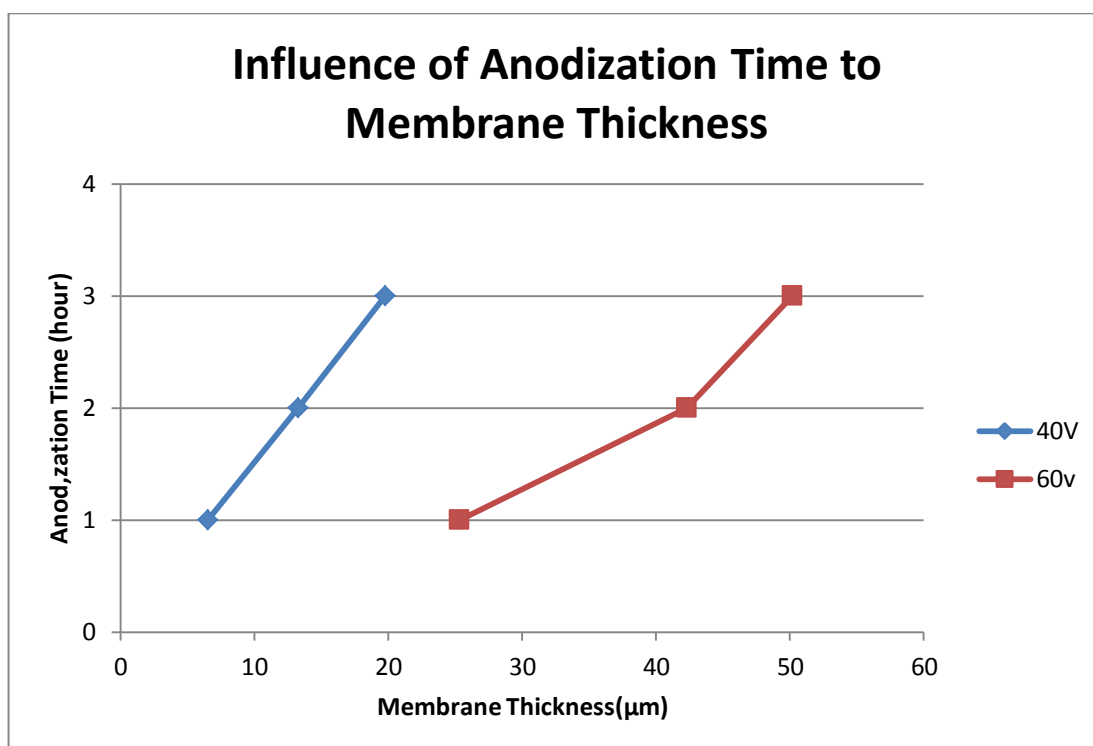


Figure 4.8: Influence of Anodization Time to Membrane Thickness.

- **Influence of Stirring Speed on the Morphology**

To examine the influence of stirring speed to morphology, we produced three two-step anodization samples at three different stirring speed; 100, 500, 900 rpm (Figure 4.9, Figure 4.10, Figure 4.11 and Figure 4.12).

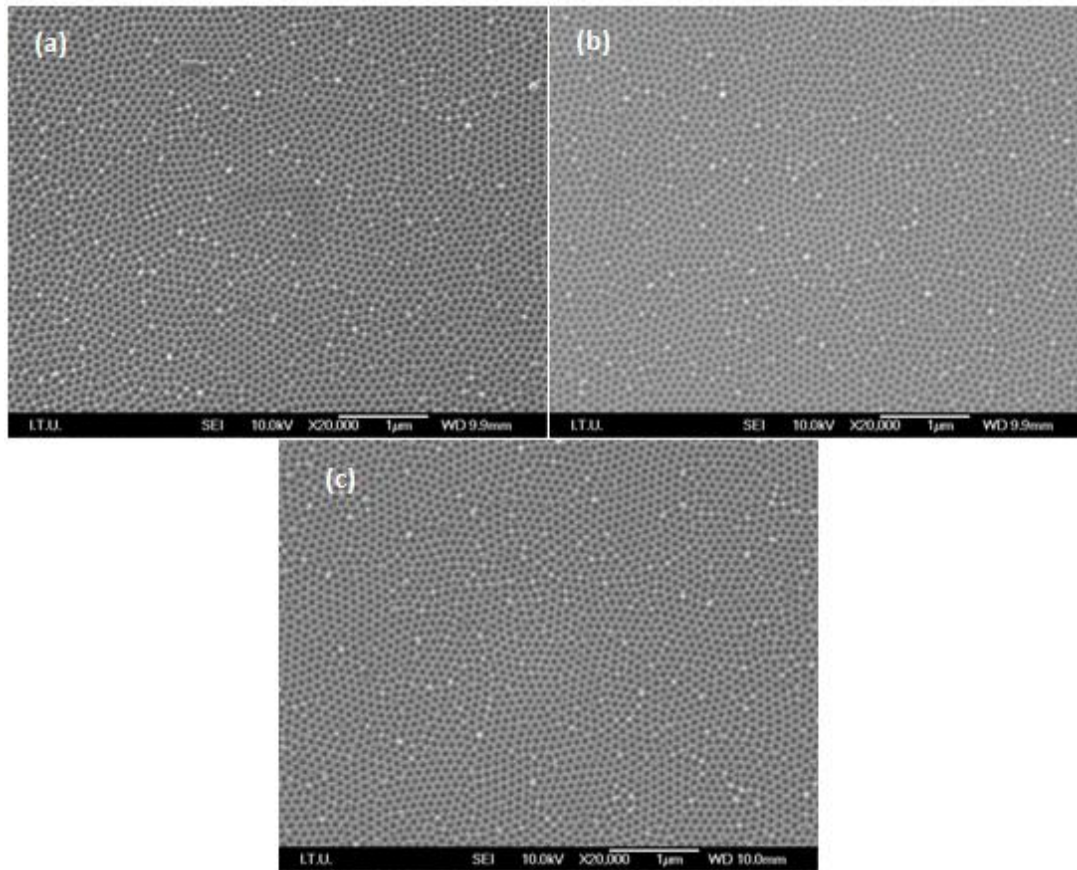


Figure 4.9: FEG-SEM image of NPAA membrane under the second anodization in 0.3 M $C_2H_2O_4$ for 5 min. at (a) 100 rpm, (b) 500 rpm, (c) 900 rpm.

SEM analysis show that with the decreasing stirring speeds, morphology becomes less homogenous and pore radius, wall thickness and interpore distance are growing.

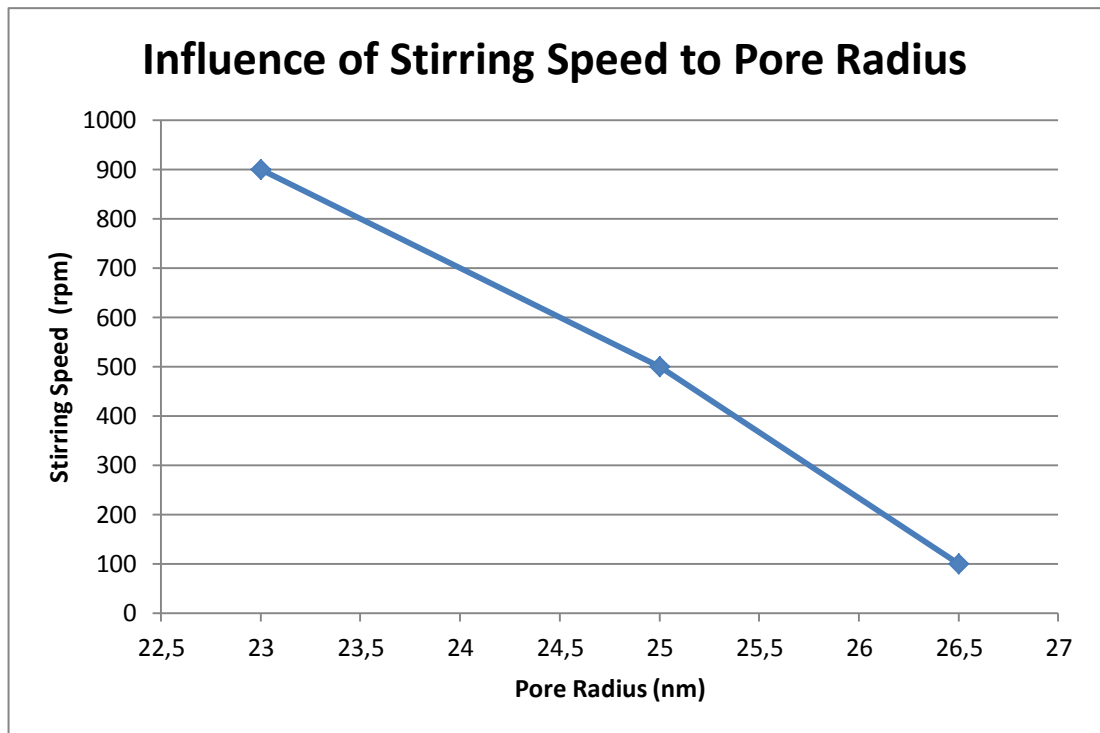


Figure 4.10: Influence of Stirring Speed to Pore Radius.

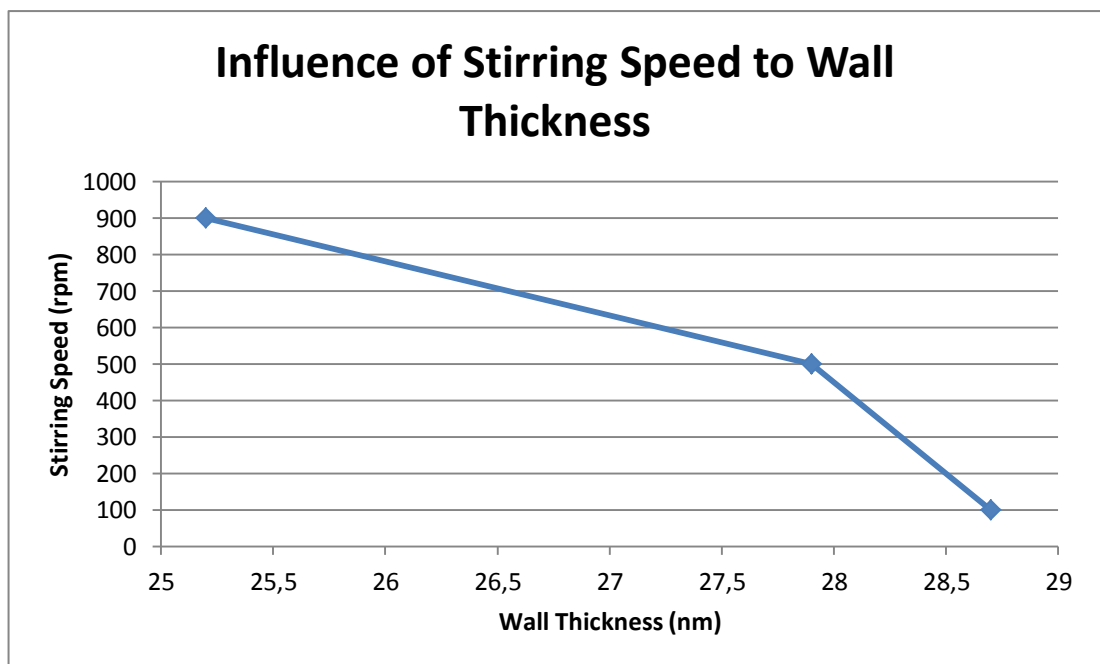


Figure 4.11: Influence of Stirring Speed to Wall Thickness.

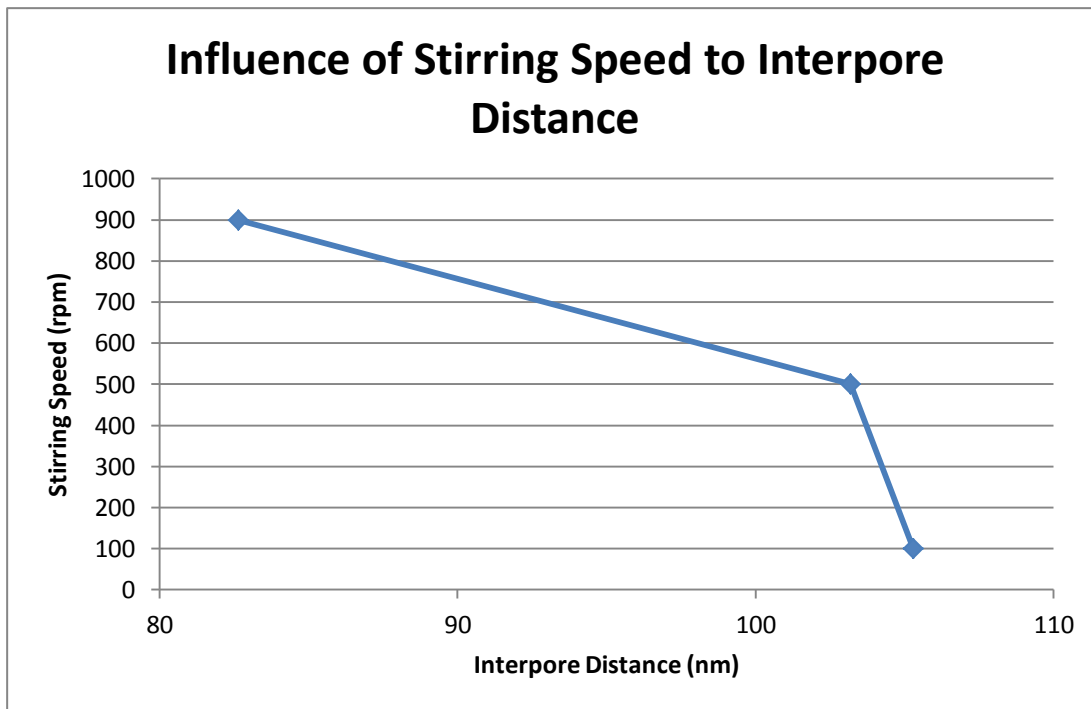


Figure 4.12: Influence of Stirring Speed to Interpore Distance.

- **Influence of Stirring Speed on the Membrane Thickness**

To examine the influence of stirring speed to membrane thickness, we produced three two-step anodization samples at three different stirring speed; 100, 500, 900 rpm.

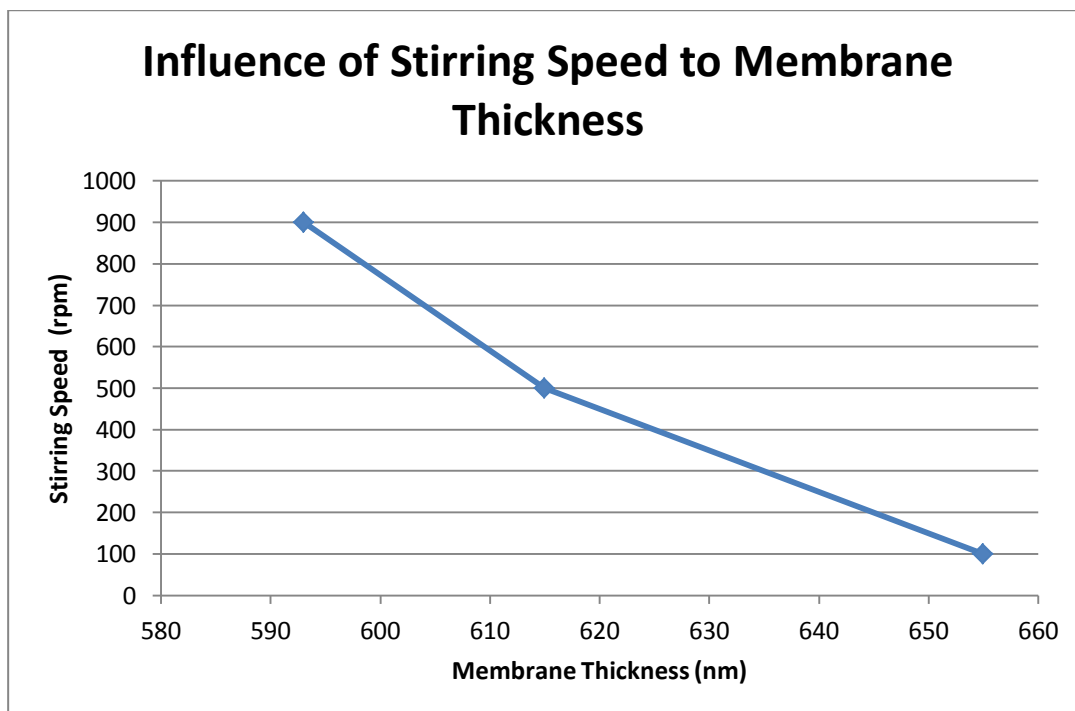


Figure 4.13: Influence of stirring Speed to Membrane Thickness.

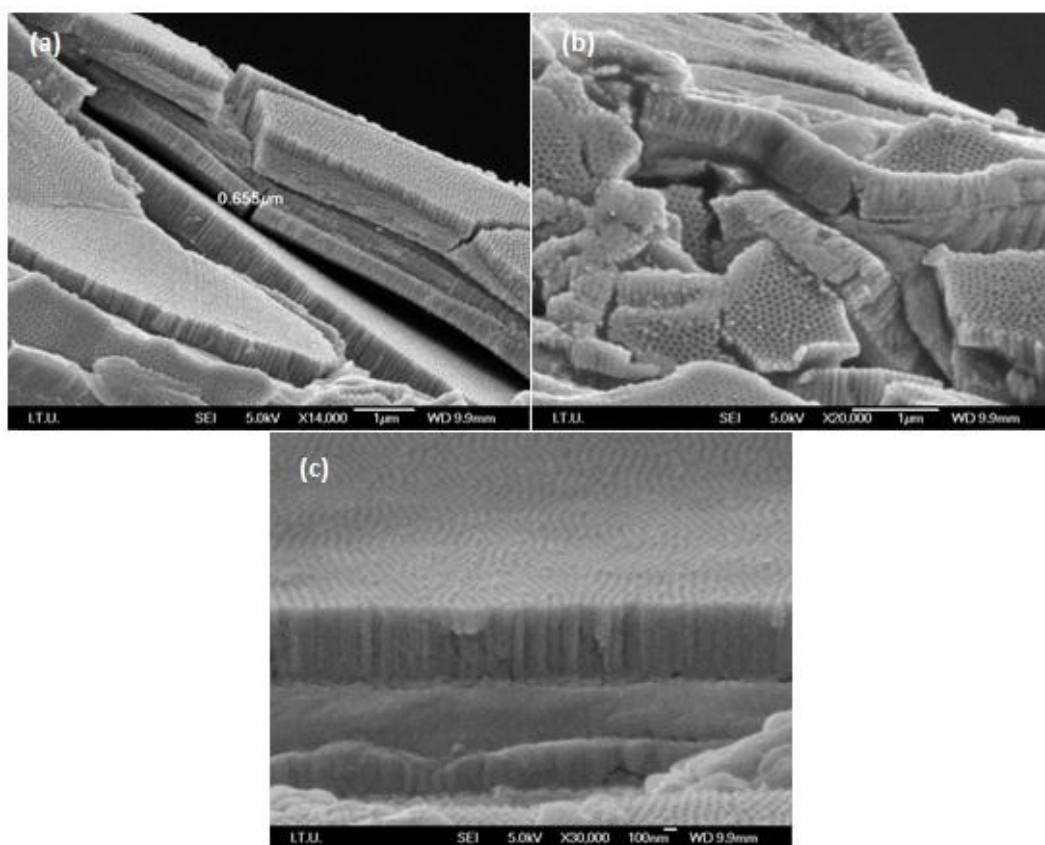


Figure 4.14: FEG-SEM cross-section image of NPAA membrane under the second anodization 0.3 M $\text{C}_2\text{H}_2\text{O}_4$ at 40 V for 5 minutes at (a) 100 rpm, (b) 500 rpm, (c) 900 rpm.

Figure 4.13 and Figure 4.14 show that with the decreasing stirring speeds, membrane is becomes thicker.

- **Effect of Etching**

To examine the effect of etching, we etched two one-step anodization samples anodized at different voltages; 40 V and 60 V.

SEM analysis shows that there are similar morphologic properties between the two surfaces and etching process doesn't make any differences between anodized samples, even if the first anodize step is realised at different potentials (Figure 4.15).

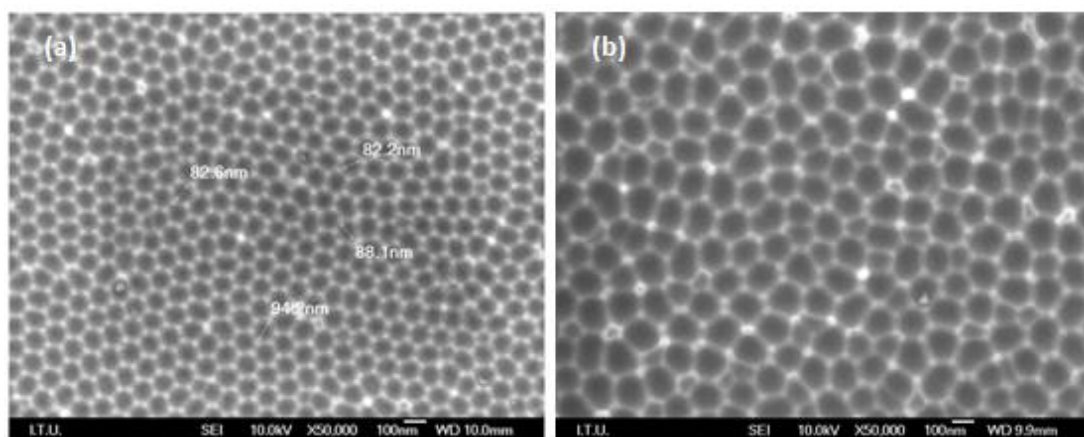


Figure 4.15: FEG-SEM image of etched AAO surface in chromic-phosphoric acid mixture for 1 hour at 60 °C at (a) 40 V, (b) 60 V.

- **Influence of Voltage on the Detachment**

We use an addition of 10 V to second anodization voltage as a constant for detachment process. To keep the surface morphology identical with the previous experiments, all samples are anodized for one hour. Thickness of membrane obtained at 40 V is thinnest and the membrane obtained at 70 V is the thickest. We examine detachment surface of three samples obtained at three different anodization voltages; 40 V, 60 V, 70 V.

SEM analysis showed that it is easier to detach the thicker membranes than the thinner ones (Figure 4-16 a-c). In the study, the samples obtained at 40 V and 50 V don't detach surface after voltage pulse and stay surface of aluminium. They required to break off to detach from aluminiums surface. On the other hand at 60 V and 70 V the membranes detach itself after voltage pulse and they fall into the detachment solution. The main differences of this causes this is the film thickness parameter. Figure 4.16 a shows that the sample that obtained at 40 V has more closed pores than the others. Also we need to break off the membranes to detach membrane because of closed pores. Moreover we discovered there are closed pores at other samples too but they are dispersed homogenously and do not prevent the membrane from detachment.

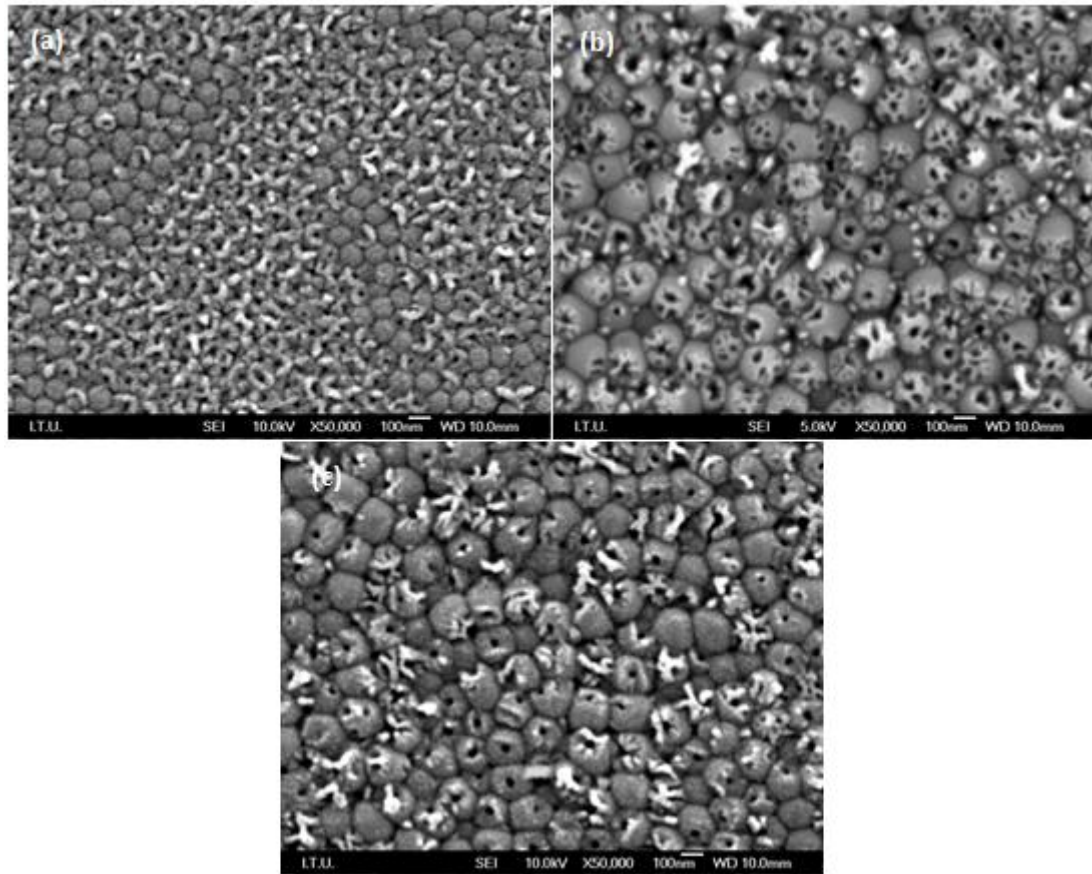


Figure 4.16: Detachment surfaces of different NPAA, these obtained at different voltages; (a) 40 V, (b) 60 V, (c) 70 V.

- **Effect of Phosphoric Acid to Detachment Surface**

We discussed previously that the detachment surface has different morphology than the top surface. The reason for this is the lack of the dissolution of barrier layer. Also barrier layer don't dissolve completely and pore don't open completely. But open-through structure can be handy at fabrication of nanostructures process. Also we used phosphoric acid to overcome this problem. We tried to dissolve the remained barrier layer with our etch solution; 0.1 M mixture of 1.8% CrO_3 and 7.1% H_3PO_4 . SEM analysis show that 5 minutes etching is enough to obtain ordered open open-through pore structure (Figure 4.17).

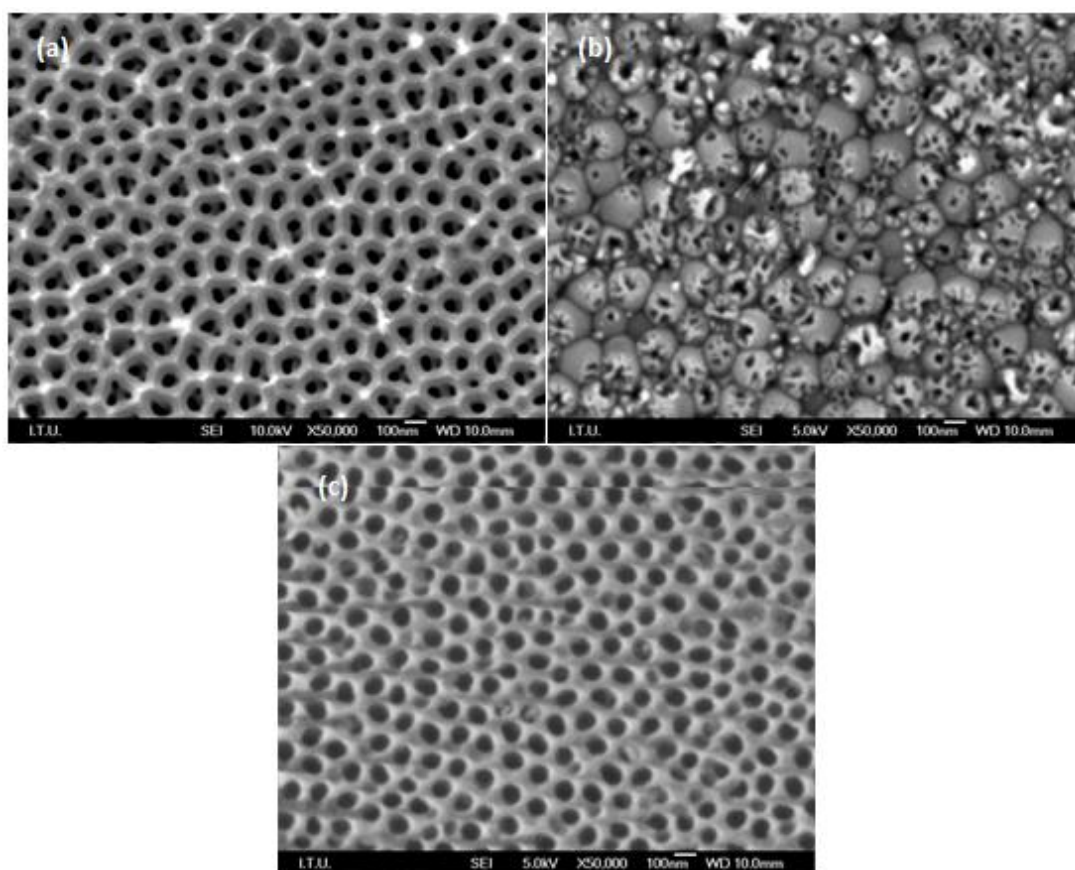


Figure 4.17: Two-step anodized samples at 60 V for one hour and detached at 70 V. (a) top surface, (b) detachment surface before etching; (c) detachment surface after etching with 0.1 M mixture of 1.8% CrO_3 and 7.1% H_3PO_4 acid for 5 minutes.

5. CONCLUSION

In our study we investigated influence of several parameters to anodization process in 0.3 M Oxalic acid and at constant temperature of 15 °C. In addition to that we investigated detachment process by using a short voltage pulse in a mixture of chloric and ethanol (volume ratio 1:1). After experiments, we reached these results;

- Second step anodization has influence upon morphology of NPAA membranes. After the second anodization pore formation become more homogenous and pore radius become larger.
- Increasing the anodization voltage results in increasing of the pore radius, interpore distance and wall thickness. Moreover pore formation become less homogenous with increasing voltage. We get most ordered formation at 40 V anodization voltage.
- Increasing the anodization time results in increasing of the membrane thickness. Increasing ratio of the membrane thickness becomes bigger by increasing the applied voltage.
- Increasing the stirring speed results in decreasing of the pore radius, interpore distance, wall thickness and membrane thickness. Moreover pore formation becomes more homogenous with increase stirring speed.
- Potential difference in the first anodization step has no effect upon etched surface morphology.
- Second anodization of membranes at 40 and 50 V for one hour is not enough to detach these membranes by short voltage pulse. They should be anodized for more time i.e. 3 hours.
- Second anodization of membranes at 60 and 70 V for one hour is enough to detach these membranes by short voltage pulse.
- Increasing anodization voltage up to 70 V resulted with better detachment.
- In 0.1 M mixture of 1.8% CrO₃ and 7.1% H₃PO₄ solution, 5 minutes is enough to open pores of detachment surface.

We obtained extensive data to fabricate NPAA membranes with desired pore radius, wall thickness, interpore radius, membrane thickness and open-through pores. We will use these membranes to fabricate one-dimensional nanostructures such as nanowires.

REFERENCES

- Bhushan, B.**, (2010). Springer Handbook of Nanotechnology 3rd ed.
- Choi, J.**, 2004, Fabrication of Monodomain Porous Alumina Using Nanoimprint Lithography and Its Applications, PhD.Thesis, Martin-Luther- Universitat Halle, Wittenberg, Germany
- Chu, S. Z.; Wada, K.; Inoue, S.; Isoqai, M.; Katsuta, Y.; Yasumori, A.**, (2006). Large-Scale Fabrication of Ordered Nanoporous Alumina Films with Arbitrary Pore Intervals by Critical-Potential Anodization. *J. Electrochem. Soc.* **153**, B384–B391.
- Chung, C. K., Liao, M. W., Chang, H. C., & Lee, C. T.**, (2011). Effects of temperature and voltage mode on nanoporous anodic aluminium oxide films by one-step anodization. *Thin Solid Films*, **520**(5), 1554-1558. Elsevier B.V. doi:10.1016/j.tsf.2011.08.053
- Ebihara, K., Takahashi, H., Nagayama, M.**, (1983) Structure and density of anodic aluminium in oxalic acid solutions, *J. Met. Finish. Soc. Japan* **34**, 548–553.
- Erdogan, P., Yuksel, B., & Birol, Y.**, (2012). Effect of chemical etching on the morphology of anodic aluminum oxides in the two-step anodization process. *Applied Surface Science*, **258**(10), 4544-4550. Elsevier B.V. doi:10.1016/j.apsusc.2012.01.025
- Hamrakulov, B., Kim, I.-S., Lee, M. G., & Park, B. H.**, (2009). Electrodeposited Ni, Fe, Co and Cu single and multilayer nanowire arrays on anodic aluminum oxide template. *Transactions of Nonferrous Metals Society of China*, **19**, s83-s87. The Nonferrous Metals Society of China. doi:10.1016/S1003-6326(10)60250-6
- Han, X. Y., & Shen, W. Z.**, (2011). Improved two-step anodization technique for ordered porous anodic aluminum membranes. *Journal of Electroanalytical Chemistry*, **655**(1), 56-64. doi:10.1016/j.jelechem.2011.02.008
- Huh, S.H., Riu, D.H., Choi, J., Kim, S.J., Jin, E.J., Shin, D.G. and Cho, K.Y.**, 2007, Surface and bottom structures of grouped alumina nanopores, *Journal of the Korean Physical Society*, **51**, pp. L1-L3
- Hwang, S.K., Jeong, S.H., Hwang, H.Y., Lee, O.J., Lee, K.H.**, (2002). Fabrication of Highly Ordered Pore. Array in Anodic Aluminum Oxide, *Korean J. Chem. Eng.*, (19) 467–473.
- Keller, F., Hunter, M. S. and Robinson, D. L.**, (1953). Structural Features of Oxide

- Coatings on Aluminum, *Journal of Electrochemical Society*, 100, 411-419
- Ko, S., Lee, D., Jee, S., Park, H., Lee, K., & Hwang, W.,** (2006). Mechanical properties and residual stress in porous anodic alumina structures. *Thin Solid Films*, 515(4), 1932-1937. doi:10.1016/j.tsf.2006.07.169
- Kyotani, T., Xu, W. H., Yokoyama, Y., Inahara, J., Touhara, H., Tomita, A.,** (2002) Chemical modification of carbon-coated anodic alumina films and their application to membrane filter, *Journal of Membrane Science*, (196), 231–239.
- Li, F., Zhang, L., & Metzger, R. M.,** (1998). On the Growth of Highly Ordered Pores in Anodized Aluminum Oxide, 4756(28), 2470-2480.
- Nash N., P., Alloys, N., Nash, P.,** (1991). Cu-Ni. *Material Park* 85-95.
- Nielsch, K., Choi, J., Schwirn, K., Wehrspohn, R. B., and Gösele U.,** (2002). Self-ordering regimes of porous alumina: The 10% porosity rule, *Nano Letters*, (2) 677-680.
- O’Sullivan, J. P., & Wood, G. C.,** (1970). The Morphology and Mechanism of Formation of Porous Anodic Films on Aluminium. *Proceedings of the Royal Society A: Mathematical, Physical and Engineering Sciences*, 317(1531), 511-543. doi:10.1098/rspa.1970.0129
- Pasaoglu, I.,** (2011) Electrodeposition and Characterization of Free Standing Ni-W Nanowires on Anodized Aluminum Oxide Templates, MSc.Thesis, Istanbul Technical University, Istanbul, Turkey
- Palibroda, E.,** (1984). *Surf. Technol.*, (23) 341–351 (in French).
- Paolini, G., Masoero, M., Sacchi, F., & Paganelli, M.,** (1965). An Investigation of Porous Anodic Oxide Films on Aluminum by Comparative Adsorption, Gravimetric and Electronoptical Measurements. *Journal of The Electrochemical Society*, 112(1), 32. doi:10.1149/1.2423460
- Parkhutik, V.P., Shershulsky, V.I.,** (1992). Theoretical modelling of porous oxide growth on aluminium, *J. Phys. D: Appl. Phys.*, 25, 1258– 1263.
- Patermarakis, G., Chandrinos, J., & Masavetas, K.,** (2007). Formulation of a holistic model for the kinetics of steady state growth of porous anodic alumina films. *Journal of Solid State Electrochemistry*, 11(9), 1191-1204. doi:10.1007/s10008-006-0259-z
- Poinern, G. E. J., Ali, N., & Fawcett, D.,** (2011). Progress in Nano-Engineered Anodic Aluminum Oxide Membrane Development *Materials* (Vol. 4, pp. 487-526). doi:10.3390/ma4030487
- Sulka, G. D.,** (2008). Highly Ordered Anodic Porous Alumina Formation Anodizing
- Sulka, G.D., Parkova, K.G.,** (2007). Temperature influence on well-ordered nanopore structures grown by anodization of aluminium in sulphuric acid, *Electrochim. Acta*, 52, 1880–1888.

- Sui, Y.,** (2001). Characterization of anodic porous alumina by AFM, (April), 127-136.
- Thompson, G.E.,** (1997). *Thin Solid Films*, 297, 192–201
- Thompson, G.E.,** Wood, G.C. (1983). Treatise on Materials Science and Technology, *Academic Press New York*, 23, 205–329
- Wernick, S., Pinner, R., Sheasby, P.G.,** (1987). The Surface Treatment and Finishing of Aluminium and its Alloys, *ASM International*, FinishingPublication Ltd., 5th edition, 289–368.
- Wood, G.C., O’Sullivan, J.P., Vaszko, B.,** (1968). The direct observation of barrier layers in porous anodic oxide films, *Journal of Electrochemical Society*, 115, 618-620.
- Wu, Z., Richter, C., & Menon, L.,** (2007). A Study of Anodization Process during Pore Formation in Nanoporous Alumina Templates. *Journal of The Electrochemical Society*, 154(1), E8. doi:10.1149/1.2382671
- Xu, T. T., Piner, R. D., & Ruoff, R. S.,** (2003). An Improved Method To Strip Aluminum from Porous Anodic Alumina Films, 80(19), 1443-1445.
- Yuan, J. H., He, F. Y., Sun, D. C., & Xia, X. H.,** (2004). A Simple Method for Preparation of Through-Hole Porous Anodic Alumina, 131(19), 1841-1844.
- Zhou, J.-hua, He, J.-ping, Zhao, G.-wang, Zhang, C.-xiang, Zhao, J.-shuang, & Hu, H.-ping.,** (2007). Alumina nanostructures prepared by two-step anodization process. *Transactions of Nonferrous Metals Society of China*, 17(1), 82-86. doi:10.1016/S1003-6326(07)60052-1
- Url-1** <<http://www.quantum3.co.za/CI%20Glossary.htm>> accessed at 10.06.2012
- Url-2** <<http://www.whatman.com/products.aspx?PID=193>> accessed at 10.06.2012
- Url-3** <<http://electrochem.cwru.edu/encycl/art-a02-anodizing.htm>> accessed at 10.06.2012

CURRICULUM VITAE

Name Surname: Emek Göksu DURMUŞOĞLU

Place and Date of Birth: Istanbul 16/04/1986

Address: 1.cad 2.sok no:16 B-236 Acarkent Kavacık/ Istanbul

E-Mail: emek.durmusoglu@gmail.com

B.Sc.: Yıldız Technical University Metallurgy and Material Engineering

M.Sc: Istanbul Technical University Nanoscience and Nanoengineering

